Two Higgs doublets, a 4th generation and a 125 GeV Higgs: a review

Shaouly Bar-Shalom,[1, *] Michael Geller,[1, †] Soumitra Nandi,[2, ‡] and Amarjit Soni[3, §]

[1]*Physics Department, Technion-Institute of Technology, Haifa 32000, Israel*
[2]*Theoretische Elementarteilchenphysik, Naturwissenschaftlich Technische Fakultät,*
Universität Siegen, 57068 Siegen, Germany
[3]*Theory Group, Brookhaven National Laboratory, Upton, NY 11973, USA*
(Dated: October 27, 2018)

We review the possible role that multi-Higgs models may play in our understanding of the dynamics of a heavy 4th sequential generation of fermions. We describe the underlying ingredients of such models, focusing on two Higgs doublets, and discuss how they may effectively accommodate the low energy phenomenology of such new heavy fermionic degrees of freedom. We also discuss the constraints on these models from precision electroweak data as well as from flavor physics and the implications for collider searches of the Higgs particles and of the 4th generation fermions, bearing in mind the recent observation of a light Higgs with a mass of ~ 125 GeV.

Invited Review:
to appear in a special issue of Advances in High Energy Physics (AHEP) on Very Heavy Quarks at the LHC

*Electronic address: shaouly@physics.technion.ac.il
†Electronic address: mic.geller@gmail.com
‡Electronic address: soumitra.nandi@gmail.com
§Electronic address: soni@bnl.gov

I. INTRODUCTION - THE "NEED" OF A MULTI-HIGGS SETUP FOR THE 4TH GENERATION

The minimal and perhaps the simplest framework for incorporating 4th generation fermions can be constructed by adding to the Standard Model (SM) a 4th sequential generation of fermion (quarks and leptons) doublets (for reviews see [1–3]). This framework, which is widely known as the SM4, can already address some of the leading theoretical challenges in particle physics:

- The hierarchy problem [4–7].

- The origin of matter - anti matter asymmetry in the universe [8, 9].

- Flavor physics and CKM anomalies [10–14].

Unfortunately, the current bounds on the masses of the 4th generation quarks within the SM4 are rather high - reaching up to ~ 600 GeV [15–18], i.e., around the unitarity bounds on quark masses [19]. The implications of such a "super-heavy" 4th generation spectrum are far reaching. In fact, the SM4 as such is also strongly disfavored from searches at the LHC [20, 21] and Tevatron [22] of the single Higgs particle of this model, essentially excluding the SM4 Higgs with masses up to 600 GeV [23] and, thus, making it incompatible with the recent observation/evidence of a light Higgs with a mass of ~ 125 GeV [24, 25] (for a recent comprehensive analysis of the SM4 status in light of the latest Higgs results and electroweak precision data (EWPD), we refer the reader to [26]). These rather stringent limits on the SM4 raise several questions at the fundamental level:

1. Are super-heavy fermionic degrees of freedom a surprise or is that expected once new physics (NP), beyond the SM4 (BSM4), is assumed to enter at the TeV-scale?

2. Are such heavy fermions linked to strong dynamics and/or to compositeness at the near by TeV-scale?

3. What sub-TeV degrees of freedom should we expect if indeed such heavy fermions are found? and what is the proper framework/effective theory required to describe the corresponding low energy dynamics?

4. How do such heavy fermions effect Higgs physics?

5. Can one construct a natural framework for 4th generation heavy fermions with a mass in the range $400 - 600$ GeV that is consistent with EWPD and that is not excluded by the recent direct measurements from present high energy colliders?

6. What type of indirect hints for BSM4 dynamics can we expect in low energy flavor physics?

In this article we will try to address these questions by considering a class of BSM4 low energy effective theories which are based on multi-Higgs models.

Let us start by studying the hints for BSM4 and strong dynamics from the evolution of the 4th generation Yukawa coupling y_4, under some simplifying assumptions. In particular, one can write the RGE of y_4 assuming SM4 dynamics and neglecting the gauge and the top-Yukawa couplings and taking all 4th generation Yukawa couplings equal [27]:

$$\left(16\pi^2\right)\mu\frac{\partial}{\partial\mu}y_4 \simeq (2y_4)^3 \tag{1}$$

This yields a Landau Pole (defined by $1/y_4^2(\mu = \Lambda_y) \to 0$) at $\Lambda_y \simeq m_4 e^{\frac{\pi^2 v^2}{2m_4^2}}$, giving $\Lambda_y \sim 8, 3, 2$ TeV for $m_4 \sim 300, 400, 500$ GeV. Therefore, within the SM4, the 4th generation Yukawa couplings are expected to "run into" a Landau Pole at the near by TeV-scale.

In fact, there are additional strong indications from the Higgs sector that a heavy 4th generation of fermions is tied with new strong dynamics at the near by TeV-scale and that the SM4 is not the adequate framework to describe the new TeV-scale physics:

1. **The Higgs mass correction due to such heavy fermions is pushed to the cutoff scale:**
   To see that, one can calculate the self-energy 1-loop correction to the Higgs mass with the exchange of a heavy fermion q' and set the cutoff to $\Lambda > m_{q'}$, obtaining:

$$\delta m_H^2 \sim \left(\frac{m_{q'}}{400 \text{ GeV}}\right)^2 \cdot \Lambda^2 , \tag{2}$$

   indicating that a heavy 4th family fermion with a mass around 400 GeV cannot co-exist with the recently observed single light Higgs, since in the absence of fine tuning, the Higgs mass should be pushed up to the cutoff scale where the NP enters (in which case the definition of the Higgs particle becomes meaningless).

2. **The SM4 Higgs quartic coupling (λ) and a heavy Higgs:**
   One can again study the RGE for λ, assuming SM4 dynamics and neglecting the gauge and the top-Yukawa couplings and taking all 4th generation Yukawa couplings equal. One then obtaines [27]:

$$\left(16\pi^2\right)\mu\frac{\partial}{\partial\mu}\lambda \simeq 24\lambda^2 + 16y_4^2\left(2\lambda - y_4^2\right)\theta(\mu - m_4)\ , \tag{3}$$

giving a Landau Pole (i.e., $\lambda(\mu = \Lambda_\lambda) \to \infty$) at $\Lambda_\lambda \sim 4.3, 2.5, 2.1$ TeV for $m_H \sim 500,\ 600,\ 700$ GeV and, thus, indicating that a light Higgs is not consistent with the SM4 if the NP scale is at the few TeV range. Indeed, solving the full RGE for the SM4 one finds that $m_H \gtrsim m_{q'}$ when the cutoff of the theory is set to the TeV-scale, i.e., to the proper cutoff of the SM4 when $m_{q'} \sim \mathcal{O}(500)$ GeV [27]. The implications of a heavy Higgs in this mass range was considered e.g., in [28–31], claiming that the heavy SM4 Higgs case can relax the currently reported exclusion on the SM4. However, the heavy SM4 Higgs scenario is now in contradiction with the recent measurements of the two experiments at the LHC, which observe a light Higgs boson with a mass of ~ 125 GeV [20, 21]. On the other hand, as will be shown in this paper (and was also demonstrated before in [27] for the case of the popular 2HDM of type II with a 4th generation of doublets), a multi-Higgs setup for the 4th generation theory can relax the constraint $m_H \gtrsim m_{q'}$.

Thus, under the assumption that heavy 4th generation quarks exist, if one assumes a light Higgs with a mass around 125 GeV and seriously takes into account the fact that low energy 4th generation theories posses a new threshold/cutoff (or a fixed point, see e.g., [32, 33]) at the TeV-scale, then one is forced to consider extensions of the naive SM4 with more than one Higgs doublet which, in turn, leads to the possibility that the Higgs particles (or some of the Higgs particles) may be composites primarily of the 4th generation fermions (see e.g., [34–38]), with condensates $< Q'_L t'_R > \neq 0$, $< Q'_L b'_R > \neq 0$ (and possibly also $< L'_L \nu'_R > \neq 0$, $< L'_L \tau'_R > \neq 0$). These condensates then induce EWSB and generate a dynamical mass for the condensing fermions. This viewpoint in fact dates back to an "old" idea suggested more than two decades ago [4]; that a heavy top-quark may be used to form a $t\bar{t}$ condensate which could trigger dynamical EWSB. Although, this top-condensate mechanism led to the prediction of a too large m_t, this idea ignited further thoughts and studies towards the possibility that 4th generation fermions may play an important role in dynamical EWSB [4, 5]. In particular, due to the presence of such heavy fermionic degrees of freedom, some form of strong dynamics and/or compositeness may occur at the near by TeV-scale.

In this article, we will review the above viewpoint which was also adopted in Ref. [39]: that theories which contain such heavy fermionic states are inevitably cutoff at the near by TeV-scale, and are, therefore, more naturally embedded at low energies in multi-Higgs models, which are the proper low-energy effective frameworks for describing the sub-TeV dynamics of 4th generation fermions. As mentioned above, in this picture, the Higgs particles are viewed as the composite scalars that emerge as manifestations of the different possible bound states of the fundamental heavy fermions. This approach was considered already 20 years ago by Luty [40] and more recently in [38], where an attempt to put 4th degeneration heavy fermions into an effective multi (composite) Higgs doublets model was made, using a Nambu-Jona-Lasinio (NJL) type approach.

The phenomenology of multi-Higgs models with a 4th family of fermions was studied to some extent recently in [27, 41–47] and within a SUSY framework in [9, 48–50]. In this article, we will further study the phenomenology of 2HDM frameworks with a 4th family of fermions, focusing on a new class of 2HDM's "for the 4th generation" (named hereafter 4G2HDM) that can effectively address the low-energy phenomenology of a TeV-scale dynamical EWSB scenario, which is possibly triggered by the condensates of the 4th generation fermions.

We will first describe a few viable manifestations of a 2HDM framework with a 4th generation of fermions, focusing on the 4G2HDM framework of Ref. [39]. We will then discuss the constraints on such 4th generation 2HDM models from PEWD as well as from flavor physics. We will end by studying the expected implication of such 2HDM frameworks on direct searches for the 4th generation fermions and for the Higgs particle(s), assuming the existence of a light Higgs with a mass of 125 GeV.

II.   2HDM'S AND 4TH GENERATION FERMIONS

Assuming a common generic 2HDM potential, the phenomenology of 2HDM's is generically encoded in the texture of the Yukawa interaction Lagrangian. The simplest variant of a 2HDM with 4th generations of fermions, can be constructed based on the so called type II 2HDM (which we denote hereafter by 2HDMII), in which one of the Higgs doublets couples only to up-type fermions and the other to down-type ones. This setup ensures the absence of tree-level flavor changing neutral currents (FCNC) and is, therefore, widely favored when confronted with low energy flavor data. The Yukawa terms of the 2HDMII, extended to include the extra 4th generation quark doublet is (and

similarly in the leptonic sector):

$$\mathcal{L}_Y = -\bar{Q}_L \Phi_d F_d d_R - \bar{Q}_L \tilde{\Phi}_u F_u u_R + h.c. , \tag{4}$$

where $f_{L(R)}$ are left(right)-handed fermion fields, Q_L is the left-handed $SU(2)$ quark doublet and F_d, F_u are general 4×4 Yukawa matrices in flavor space. Also, $\Phi_{d,u}$ are the Higgs doublets:

$$\Phi_i = \begin{pmatrix} \phi_i^+ \\ \frac{v_i + \phi_i^0}{\sqrt{2}} \end{pmatrix}, \quad \tilde{\Phi}_i = \begin{pmatrix} \frac{v_i^* + \phi_i^{0*}}{\sqrt{2}} \\ -\phi_i^- \end{pmatrix} ,$$

Motivated by the idea that the low energy scalar degrees of freedom may be the composites of the heavy 4th generation fermions, it is possible to construct a new class of 2HDM's that effectively parameterize 4th generation condensation by giving a special status to the 4th family fermions. This was done in [39], where (in the spirit of the Das and Kao 2HDM that was based on the SM's three families of fermions [51]) one of the Higgs fields (ϕ_h - call it the "heavier" field) was assumed to couple only to heavy fermionic states, while the second Higgs field (ϕ_ℓ - the "lighter" field) is responsible for the mass generation of all other (lighter) fermions. The possible viable variants of this approach can be parameterized as [39] (and similarly in the leptonic sector):

$$\mathcal{L}_Y = -\bar{Q}_L \left(\Phi_\ell F_d \cdot \left(I - \mathcal{I}_d^{\alpha_d \beta_d} \right) + \Phi_h F_d \cdot \mathcal{I}_d^{\alpha_d \beta_d} \right) d_R - \bar{Q}_L \left(\tilde{\Phi}_\ell F_u \cdot \left(I - \mathcal{I}_u^{\alpha_u \beta_u} \right) + \Phi_h F_u \cdot \mathcal{I}_u^{\alpha_u \beta_u} \right) u_R + h.c. , \tag{5}$$

where $\Phi_{\ell,h}$ are the two Higgs doublets, I is the identity matrix and $\mathcal{I}_q^{\alpha_q \beta_q}$ ($q = d, u$) are diagonal 4×4 matrices defined by $\mathcal{I}_q^{\alpha_q \beta_q} \equiv \mathrm{diag}(0, 0, \alpha_q, \beta_q)$.

The Yukawa interaction Lagrangian of (5) can lead to several interesting textures that can be realized in terms of a Z_2-symmetry under which the fields transform as follows:

$$\begin{aligned}
&\Phi_\ell \to -\Phi_\ell, \ \Phi_h \to +\Phi_h, \ Q_L \to +Q_L, \\
&d_R \to -d_R \ (d = d, s), \ u_R \to -u_R \ (u = u, c), \\
&b_R \to (-1)^{1+\alpha_d} b_R, \ b'_R \to (-1)^{1+\beta_d} b'_R, \\
&t_R \to (-1)^{1+\alpha_u} t_R, \ t'_R \to (-1)^{1+\beta_u} t'_R ,
\end{aligned} \tag{6}$$

which allows us to construct several models that have a non-trivial Yukawa structure and that are potentially associated with the compositeness scenario:

- **type I 4G2HDM**: denoted hereafter by **4G2HDMI** and defined by $(\alpha_d, \beta_d, \alpha_u, \beta_u) = (0, 1, 0, 1)$, in which case Φ_h gives masses only to t' and b', while Φ_ℓ generates masses for all other quarks (including the top-quark). For this model, which seems to be the natural choice for the leptonic sector, we expect:

$$\tan \beta \equiv \frac{v_h}{v_\ell} \approx \frac{m_{q'}}{m_t} \sim \mathcal{O}(1) . \tag{7}$$

- **type II 4G2HDM**: denoted hereafter by **4G2HDMII** and defined by $(\alpha_d, \beta_d, \alpha_u, \beta_u) = (1, 1, 1, 1)$, in which case the heavy condensate Φ_h couples to the heavy quarks states of both the 3rd and 4th generations t and b-quarks, whereas Φ_ℓ couples to the light quarks of the 1st and 2nd generations. For this model one expects $\tan \beta \gg 1$.

- **type III 4G2HDM**: denoted hereafter by **4G2HDMIII** and defined by $(\alpha_d, \beta_d, \alpha_u, \beta_u) = (0, 1, 1, 1))$, in which case $m_t, \ m_{b'}$ and $m_{t'} \propto v_h$, so that only quarks with masses at the EW-scale are coupled to the heavy doublet Φ_h. Here also one expects $\tan \beta \gg 1$.

The Yukawa interactions for these models are given by [39]:

$$\mathcal{L}(h q_i q_j) = \frac{g}{2m_W} \bar{q}_i \left\{ m_{q_i} \frac{s_\alpha}{c_\beta} \delta_{ij} - \left(\frac{c_\alpha}{s_\beta} + \frac{s_\alpha}{c_\beta} \right) \cdot \left[m_{q_i} \Sigma_{ij}^q R + m_{q_j} \Sigma_{ji}^{q\star} L \right] \right\} q_j h , \tag{8}$$

$$\mathcal{L}(H q_i q_j) = \frac{g}{2m_W} \bar{q}_i \left\{ -m_{q_i} \frac{c_\alpha}{c_\beta} \delta_{ij} + \left(\frac{c_\alpha}{c_\beta} - \frac{s_\alpha}{s_\beta} \right) \cdot \left[m_{q_i} \Sigma_{ij}^q R + m_{q_j} \Sigma_{ji}^{q\star} L \right] \right\} q_j H , \tag{9}$$

$$\mathcal{L}(A q_i q_j) = -i I_q \frac{g}{m_W} \bar{q}_i \left\{ m_{q_i} \tan\beta \gamma_5 \delta_{ij} - (\tan\beta + \cot\beta) \cdot \left[m_{q_i} \Sigma_{ij}^q R - m_{q_j} \Sigma_{ji}^{q\star} L \right] \right\} q_j A , \tag{10}$$

$$\begin{aligned}
\mathcal{L}(H^+ u_i d_j) = \frac{g}{\sqrt{2}m_W} \bar{u}_i &\left\{ \left[m_{d_j} \tan\beta \cdot V_{u_i d_j} - m_{d_k} (\tan\beta + \cot\beta) \cdot V_{ik} \Sigma_{kj}^d \right] R \right. \\
&\left. + \left[-m_{u_i} \tan\beta \cdot V_{u_i d_j} + m_{u_k} (\tan\beta + \cot\beta) \cdot \Sigma_{ki}^{u\star} V_{kj} \right] L \right\} d_j H^+ ,
\end{aligned} \tag{11}$$

where V is the 4×4 CKM matrix, $q = d$ or u for down or up-quarks with weak Isospin $I_d = -\frac{1}{2}$ and $I_u = +\frac{1}{2}$, respectively, and $R(L) = \frac{1}{2}(1 + (-)\gamma_5)$. Also, the 4G2HDM type, i.e., the 4G2HDMI, 4G2HDMII and 4G2HDMIII, as well as FCNC effects are all encoded in Σ^d and Σ^u, which are new mixing matrices in the down(up)-quark sectors, obtained after diagonalizing the quarks mass matrices:

$$
\begin{aligned}
\Sigma^d_{ij} &= \Sigma^d_{ij}(\alpha_d, \beta_d, D_R) = \alpha_d D^\star_{R,3i} D_{R,3j} + \beta_d D^\star_{R,4i} D_{R,4j} \ , \\
\Sigma^u_{ij} &= \Sigma^u_{ij}(\alpha_u, \beta_u, U_R) = \alpha_u U^\star_{R,3i} U_{R,3j} + \beta_u U^\star_{R,4i} U_{R,4j} \ ,
\end{aligned}
\tag{12}
$$

depending on D_R, U_R which are the rotation (unitary) matrices of the right-handed down and up-quarks, respectively, and on whether α_q and/or β_q are "turned on". This is in contrast to "standard" frameworks such as the SM4 and the 2HDM's of types I and II, where the right-handed mixing matrices U_R and D_R are non-physical being "rotated away" in the diagonalization procedure of the quark masses. Indeed, in the 4G2HDM's described above some elements of D_R and U_R can, in principle, be measured in Higgs-fermion systems, as we will later show.

In particular, inspired by the working assumption of the 4G2HDM's and by the observed flavor pattern in the up and down-quark sectors, it was shown in [39] that the new mixing matrices Σ^d and Σ^u are expected to have the following form:

$$
\Sigma^u = \begin{pmatrix}
0 & 0 & 0 & 0 \\
0 & \alpha_u |\epsilon_c|^2 & \alpha_u \epsilon_c^\star \left(1 - \frac{|\epsilon_t|^2}{2}\right) & -\alpha_u \epsilon_c^\star \epsilon_t^\star \\
0 & \alpha_u \epsilon_c \left(1 - \frac{|\epsilon_t|^2}{2}\right) & \alpha_u \left(1 - \frac{|\epsilon_t|^2}{2}\right) + \beta_u |\epsilon_t|^2 & (\beta_t - \alpha_t)\epsilon_t^\star \left(1 - \frac{|\epsilon_t|^2}{2}\right) \\
0 & -\alpha_u \epsilon_c \epsilon_t & (\beta_u - \alpha_u)\epsilon_t \left(1 - \frac{|\epsilon_t|^2}{2}\right) & \alpha_u |\epsilon_t|^2 + \beta_u \left(1 - \frac{|\epsilon_t|^2}{2}\right)
\end{pmatrix},
\tag{13}
$$

and similarly for Σ^d by replacing $\alpha_u, \beta_u \to \alpha_d, \beta_d$ and $\epsilon_c, \epsilon_t \to \epsilon_s, \epsilon_b$. The new parameters ϵ_c, ϵ_t are free parameters that effectively control the mixing between the 4th generation t' and the 2nd and 3rd generation quarks c and t, respectively. Thus, A natural choice which will be adopted here in some instances is $|\epsilon_t| =\sim m_t/m_{t'}$, $|\epsilon_b| =\sim m_b/m_{b'}$ and ϵ_s, $\epsilon_c \to 0$.

III. CONSTRAINTS ON 2HDM'S WITH A 4TH GENERATION OF FERMIONS

A. Constraints from electroweak precision data: oblique parameters

The sensitivity of EWPD to 4th generation fermions within the minimal SM4 framework was extensively analyzed in the past decade [52–58]. Here we are interested instead on the constraints that EWPD impose on 2HDM's with a 4th generation family. As usual, the effects of the NP can be divided into the effects of the heavy NP which does and which does not couple directly to the ordinary SM fermions. For the former, the leading effect comes from the decay $Z \to b\bar{b}$, which is mainly sensitive to the $H^+ t'b$ and $W^+ t'b$ couplings through one-loop exchanges of H^+ and W^+ shown in Fig. 2, and which was analyzed in detail in [39].

On the other hand, the effects which do not involve direct couplings to the ordinary fermions, can be analyzed by the quantum oblique corrections to the gauge-bosons 2-point functions, which can be parameterized in terms of the oblique parameters S,T and U [59]. For the oblique parameters the effects of a 2HDM with a 4th generation are common to any variant of a 2HDM framework (including the 2HDMII and the 4G2HDMI, 4G2HDMII and 4G2HDMIII described in the previous section), since the Hff Yukawa interactions of any 2HDM do not contribute at 1-loop to the gauge-bosons self energies.

In particular, apart from the pure 1-loop Higgs exchanges, one also has to include the new contributions from t' and b' exchanges which shift the T parameter (ΔT_f) and which involve the new SM4-like diagonal coupling $Wt'b'$ as well as the $Wt'b$ and Wtb' off-diagonal vertices (see e.g., [57]):

$$
\Delta T_f = \frac{3}{8\pi s_W^2 c_W^2} \left(|V_{t'b'}|^2 F_{t'b'} + |V_{t'b}|^2 F_{t'b} + |V_{tb'}|^2 F_{tb'} - |V_{tb}|^2 F_{tb} + \frac{1}{3}F_{\ell_4 \nu_4} \right) \ ,
\tag{14}
$$

with

$$
F_{ij} = \frac{x_i + x_j}{2} - \frac{x_i x_j}{x_i - x_j}\log\frac{x_i}{x_j} \ ,
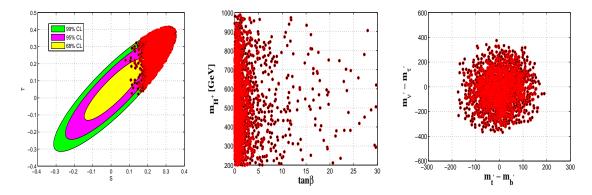\tag{15}
$$

FIG. 1: *Left plot: the allowed points in parameter space projected onto the 68%, 95% and 99% allowed contours in the S-T plane. Middle plot: 95% CL allowed range in the $m_{H^+} - \tan\beta$ plane. Right plot: allowed region in the $\Delta m_{q'} - \Delta m_{\ell'}$ plane within the 95%CL contour in the S-T plane. All plots are for any 2HDM setup (such as the 2HDMII and the three types of the 4G2HDM, see text) and with 100000 data points setting the light Higgs mass to $m_h = 125$ GeV and varying the rest of the parameters in the ranges: $\tan\beta \leq 30$, $\theta_{34} \leq 0.3$, 150 GeV $\leq m_H \leq 1$ TeV, 150 GeV $\leq m_A \leq 1$ TeV, 200 GeV $\leq m_{H^+} \leq 1$ TeV, 400 GeV $\leq m_{t'}, m_{b'} \leq 600$ GeV, 100 GeV $\leq m_{\nu'}, m_{\tau'} \leq 1.2$ TeV and the CP-even neutral Higgs mixing angle in the range $0 \lesssim \alpha \lesssim 2\pi$.*

and $x_k \equiv (m_k/m_Z)^2$.

The complete set of corrections to the S and T parameters within a 2HDM with a 4th generation of fermions was considered in [39, 53, 60]. Following the recent analysis in [39], we show in Fig. 1 the results of "blindly" (randomly) scanning the relevant parameter space with 100000 models, where we set the light Higgs mass to be $m_h = 125$ GeV and vary the rest of the relevant parameters within the ranges: $\tan\beta \leq 30$, $\theta_{34} \leq 0.3$, 150 GeV $\leq m_H \leq 1$ TeV, 150 GeV $\leq m_A \leq 1$ TeV, 200 GeV $\leq m_{H^+} \leq 1$ TeV, 400 GeV $\leq m_{t'}, m_{b'} \leq 600$ GeV, 100 GeV $\leq m_{\nu'}, m_{\tau'} \leq 1.2$ TeV, and the CP-even neutral Higgs mixing angle in the range $0 \leq \alpha \leq 2\pi$. In particular, we plot in Fig. 1 the allowed points in parameter space projected onto the 68%, 95% and 99% allowed contours in the S-T plane, the 95% CL allowed range in the $m_{H^+} - \tan\beta$ and the $\Delta m_{q'} - \Delta m_{\ell'}$ planes, corresponding to the 95%CL contour in the S-T plane

We find that compatibility with PEWD mostly requires $\tan\beta \sim \mathcal{O}(1)$ with a small number of points in parameter space having $\tan\beta \gtrsim 5$. We also find that the 2HDM frameworks allow 4th generation quarks and leptons mass splittings extended to: -200 GeV $\lesssim \Delta m_{q'} \lesssim 200$ GeV and -400 GeV $\lesssim \Delta m_{\ell'} \lesssim 400$ GeV, and "solutions" where both the quarks and the leptons of the 4th generation doublets are degenerate. For the cases of a small (or no) 4th generation fermion mass splitting, the amount of isospin breaking required to compensate for the effect of the extra fermions and Higgs particles on S and T is provided by a mass splitting among the Higgs particles, see [39].

B.   Constraints from electroweak precision data: $Z \to b\bar{b}$

The effects of the NP in $Z \to b\bar{b}$, is best studied via the well measured quantity R_b:

$$R_b \equiv \frac{\Gamma(Z \to b\bar{b})}{\Gamma(Z \to \text{hadrons})} \ , \tag{16}$$

which is a rather clean test of the SM, since being a ratio between two hadronic rates, most of the electroweak, oblique and QCD corrections cancel between numerator and denumerator.

Following [39], the effects of NP in R_b can be parameterized in terms of the corrections δ_b and δ_c to the decays $Z \to b\bar{b}$ and $Z \to c\bar{c}$, respectively:

$$R_b = R_b^{SM} \frac{1 + \delta_b}{1 + R_b^{SM}\delta_b + R_c^{SM}\delta_c} \ , \tag{17}$$

where R_b^{SM} and R_c^{SM} are the corresponding 1-loop quantities calculated in the SM, and δ_q are the NP corrections defined in terms of the $Zq\bar{q}$ couplings as:

$$\delta_q = 2\frac{g_{qL}^{SM} g_{qL}^{new} + g_{qR}^{SM} g_{qR}^{new}}{\left(g_{qL}^{SM}\right)^2 + \left(g_{qR}^{SM}\right)^2} \ , \tag{18}$$
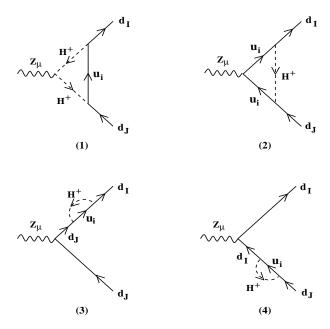
FIG. 2: *One-loop diagrams for corrections to $Z \to d_I \bar{d}_J$ from charged Higgs loops. Similar diagrams with $W - t'$ loops contribute as well.*

where

$$V_{qqZ} \equiv -i\frac{g}{c_W}\bar{q}\gamma_\mu \left(\bar{g}_{qL}L + \bar{g}_{qR}R\right)qZ^\mu \;, \tag{19}$$

with $s_W(c_W) = \sin\theta_W(\cos\theta_W)$, $L(R) = (1-(+)\gamma_5)/2$ and $\bar{g}_{qL,R} = g_{qL,R}^{SM} + g_{qL,R}^{new}$, so that $g_{qL,R}^{SM}$ are the SM (1-loop) quantities and $g_{qL,R}^{new}$ are the NP 1-loop corrections.

The corrections to R_b from the 4th generation quarks in the 4G2HDMI, 4G2HDMII and 4G2HDMIII are of three types (see [39]), where in all cases one finds that $\delta_c \ll \delta_b$, so that one can safely neglect the effects from $Z \to c\bar{c}$:
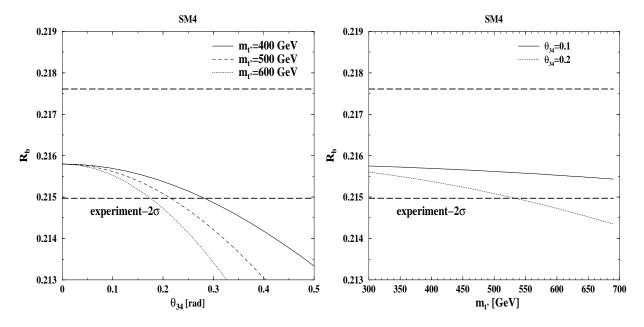

FIG. 3: *R_b in the SM4, as a function of θ_{34} for several values of the t' mass (left) and as a function of $m_{t'}$ for $\theta_{34} = 0.1$ and 0.2 (right). Figure taken from [39].*
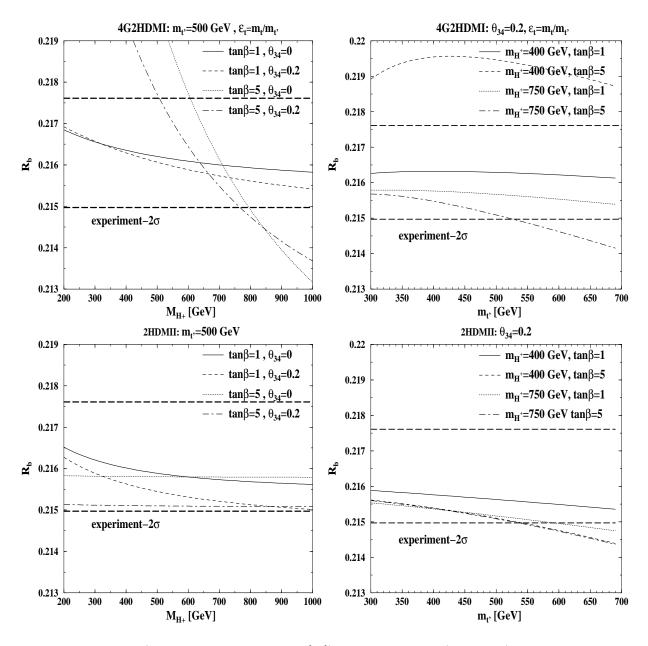
FIG. 4: R_b in the 4G2HDMI (upper plots, figure taken from [39]) and in the 2HDMII (lower plots), as a function of the charged Higgs mass (left plots) for $m_{t'} = 500$ GeV, and $(\tan\beta, \theta_{34}) = (1, 0), (1, 0.2), (5, 0), (5, 0.2)$, and as a function of $m_{t'}$ (right plots), for $\theta_{34} = 0.2$ and $(m_{H+} \text{ [GeV]}, \tan\beta) = (400, 1), (400, 5), (750, 1), (750, 5)$ (right). In the 4G2HDMI case we use $\epsilon_t = m_t/m_{t'}$. The long-dashed horizontal lines represent the upper and lower 2σ (measured) bounds on R_b.

1. **SM4-like corrections:**

These are the corrections to g_{qL} due to the 1-loop $W - t'$ exchanges (denoted here as g_{qL}^{SM4}), which are given by [11, 57, 61]:

$$g_{qL}^{SM4} = \frac{g^2}{64\pi^2 c_W^2} \left(\frac{m_{t'}^2}{m_Z^2} - \frac{m_t^2}{m_Z^2} \right) \sin^2\theta_{34} , \qquad (20)$$

where θ_{34} is the mixing angle between the 3rd and 4th generation quarks, i.e., defining $|V_{t'b}| = |V_{tb'}| \equiv \sin\theta_{34}$, and the 2nd term $\propto -\sin^2\theta_{34} m_t^2/m_Z^2$ is the decrease from the SM's tb correction to the W-boson vacuum polarization, which in the 4th generation case, is $\propto |V_{tb}|^2 = \cos^2\theta_{34} = 1 - \sin^2\theta_{34}$.
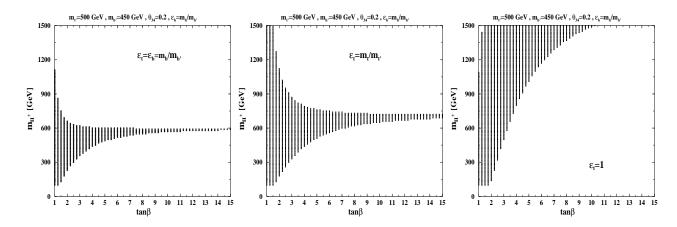
FIG. 5: *Allowed area in the $m_{H^+} - \tan\beta$ in the 4G2HDMI, subject to the R_b measurement (within 2σ), for $m_{t'} = 500$ GeV, $m_{b'} = 450$ GeV, $\theta_{34} = 0.2$, $\epsilon_b = m_b/m_{b'}$ and for three values of the $t - t'$ mixing parameter: $\epsilon_t = \epsilon_b \sim 0.01$ (left plot), $\epsilon_t = m_t/m_{t'} \sim 0.35$ (middle plot) and $\epsilon_t = 1$ (right plot). Figure taken from [39].*

The SM4-like effect on R_b is plotted in Fig. 3, from which we can see that R_b puts rather stringent constraints on the $m_{t'} - \theta_{34}$ plane which is the SM4 subspace of the parameter space of any 2HDM containing a 4th generation of fermions. For example, for $m_{t'} \sim 500$ GeV the $t' - b$ mixing angle is restricted to $\theta_{34} \lesssim 0.2$.

2. $H^+ - t'$ **exchanges:**

The corrections from the 1-loop $H^+ - t'$ exchanges are plotted in Fig. 2. In the 4G2HDM of types II and III, these charged Higgs exchange diagrams are found to have negligible effects on R_b and are, therefore, not constrained by this quantity. On the other hand, R_b is rather sensitive to the charged Higgs 1-loop exchanges within the 4G2HDMI. This can be seen in Fig. 4, where R_b is plotted (for the 4G2HDMI case) as a function of the charged Higgs and t' masses, fixing $\epsilon_t = m_t/m_{t'}$ and focusing on the values $\tan\beta = 1, 5$, $\theta_{34} = 0, 0.2$ and $m_{H^+} = 400, 750$ GeV.

In Fig. 5 we further plot the allowed ranges in the $m_{H^+} - \tan\beta$ plane in the 4G2HDMI, subject to the R_b constraint (at 2σ), for $\tan\beta$ in the range 1-15, fixing $m_{t'} = 500$ GeV, $m_{b'} = 450$ GeV, $\theta_{34} = 0.2$, $\epsilon_b = m_b/m_{b'}$ (which also enters the $t'bH^+$ vertex) and for three representative values of the $t - t'$ mixing parameter: $\epsilon_t = \epsilon_b \sim 0.01$, $\epsilon_t = m_t/m_{t'} \sim 0.35$ and $\epsilon_t = 1$. We see that, as expected, when $\tan\beta$ is lowered, the constraints on the charged Higgs mass are weakened. In particular, while there are no constraints from R_b on the charged Higgs and t' masses if $\tan\beta \sim \mathcal{O}(1)$, for higher values of $\tan\beta$ a more restricted region of the charged Higgs mass is imposed which again depends on θ_{34}. We see e.g., that for $\epsilon_t = m_t/m_{t'} \sim 0.35$, $\tan\beta \sim 1$ is compatible with m_{H^+} values ranging from 200 GeV up to the TeV scale, while for $\tan\beta \sim 5$ the charged Higgs mass is restricted to be within the range 450 GeV $\lesssim m_{H^+} \lesssim 750$ GeV.

For the case of the 2HDMII (i.e., extended with a 4th family of fermions), which is also plotted in Fig. 4, we find that there is essentially no constraint in the $m_{H^+} - \tan\beta$ plane for $m_{t'} \lesssim 500$ GeV.

3. **The flavor changing** $\mathcal{H}^0 bb'$ **interactions:**

The 1-loop Corrections to R_b which involve the flavor changing (FC) $\mathcal{H}^0 bb'$ interactions emanate from the non-diagonal 34 and 43 elements in Σ^d, with $\mathcal{H}^0 = h, H$ or A. These corrections are found to be much smaller than 1-loop H^+ exchanges, so that they can be safely neglected, in particular for $\epsilon_b \ll 1$.

C. Constraints from flavor in b-physics

1. $\bar{B} \to X_s \gamma$

Flavor physics plays an important role in discriminating between the various NP models. In this regard, FCNC decays can provide key information about the SM and its various extensions.

The inclusive radiative decay $\bar{B} \to X_s\gamma$ is indeed known to be a very sensitive probe of NP. The underlying process is induced by the FC decay of the b-quark into a strange quark and a photon. The $\text{Br}(\bar{B} \to X_s\gamma)$ has already carved out large regions of the parameter space of most of the NP models [62–65]. On the other hand, model independent analysis in the effective field theory approach without [66] and with [67] the assumption of minimal flavor violation also show the strong constraining power of the decay $\bar{B} \to X_s\gamma$. Once more precise data from Super-B factories are available, this decay will undoubtedly be more efficient in selecting the viable regions of the parameter space in the various classes of NP models.
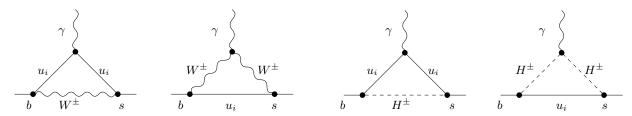

FIG. 6: *Examples of one-loop 1PI diagrams that contribute to $b \to s\gamma$ in a 2HDM framework, with W-bosons, charged Higgs and 4th generation quarks exchanges ($u_i = u, c, t, t'$).*

The calculation of the decay rate of the $\bar{B} \to X_s\gamma$ transition is most conveniently performed after integrating out the heavy degrees of freedom. The resulting effective theory contains various FC dimension-five and -six local interactions and the inclusive decay rate is given by

$$\Gamma(b \to X_s\gamma)_{E_\gamma > E_0} = \frac{G_F^2 \, m_b^5 \, \alpha_{em}}{32 \, \pi^4} |V_{ts}^* V_{tb}|^2 \sum_{i,j=1}^{8} C_i(\mu_b) \, C_j(\mu_b) G_{ij}(E_0, \mu_b), \tag{21}$$

where the Wilson coefficients, C_i, of the effective operators (see below) are perturbatively calculable at the relevant renormalization scale and the Renormalization Group Equations (RGE) can be used to evaluate C_i at the scale $\mu_b \sim m_b/2$. At present, all the relevant Wilson coefficients $C_i(\mu_b)$ are known at the Next-to-Next-to-Leading-Order (NNLO) [68–75] and $G_{ij}(E_0, \mu_b)$ is determined by the matrix elements of the operators $O_1, ..., O_8$ [76]:

$$
\begin{aligned}
O_{1,2} &= (\bar{s}\Gamma_i c)(\bar{c}\Gamma_i' b), & &\text{(current-current operators)} \\
O_{3,4,5,6} &= (\bar{s}\Gamma_i b)\textstyle\sum_q(\bar{q}\Gamma_i' q), & &\text{(four-quark penguin operators)} \\
O_7 &= \frac{em_b}{16\pi^2} \bar{s}_L\sigma^{\mu\nu}b_R F_{\mu\nu}, & &\text{(photonic dipole operator)} \\
O_8 &= \frac{gm_b}{16\pi^2} \bar{s}_L\sigma^{\mu\nu}T^a b_R G_{\mu\nu}^a. & &\text{(gluonic dipole operator)}
\end{aligned}
\tag{22}
$$

which consists of perturbative and non-perturbative corrections. The perturbative corrections are well under control and are fully known at NLO QCD [77]. However, quantitative estimates of all the non-perturbative effects are not available, although they are believed to be $\approx 5\%$ [77].

The inclusive branching ratio in the SM is given by [78]:

$$\mathcal{B}(\bar{B} \to X_s\gamma)_{E_\gamma > 1.6 \, \text{GeV}}^{NNLO} = (3.15 \pm 0.23) \times 10^{-4}, \tag{23}$$

whereas the current experimental data gives [79]:

$$\mathcal{B}(\bar{B} \to X_s\gamma)_{E_\gamma > 1.6 \, \text{GeV}}^{exp} = (3.55 \pm 0.24 \pm 0.09) \times 10^{-4}. \tag{24}$$

The SM prediction is, thus, consistent with the experiment (both having a 7% error) and is therefore useful for constraining many extensions of the SM.

In the SM4 there are no new operators other than the ones present in the SM. However, there are extra contributions to the Wilson coefficients corresponding to the operators O_7 and O_8 from t'-loops [10–13]. In a 2HDM framework with a 4th generation family, the new ingredient with respect to the SM4 is the presence of the charged Higgs 1-loop exchanges which contribute to the Wilson coefficients of the effective theory. In particular, at the parton level within a 2HDM, $\bar{B} \to X_s\gamma$ proceeds via the penguin diagrams depicted in Fig. 6. As was shown in [39], in the 4G2HDMI, 4G2HDMII and 4G2HDMIII frameworks, the leading effects enter in C_7 and C_8 from the 1-loop exchanges of $t' - W$, $t - H^+$ and $t' - H^+$.
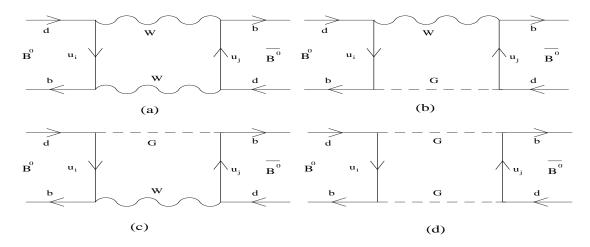
FIG. 7: *The $B^0 - \bar{B}^0$ (representative) box diagrams with different combinations of the gauge bosons (W, G) and the fermions (u_i, u_j) in the internal lines. The same diagrams contribute to $B^s - \bar{B}^s$ mixing with the d-quark in the external lines replaced by the s-quark.*

2. $B_q - \bar{B}_q$ mixing

An important role for constraining NP in the b-quark system is also played by $B_q - \bar{B}_q$ $(q = d, s)$ mixing, the phenomenon of which is described by the dispersive part M_{12}^q of the B_q mixing amplitude. The current theory precision is limited by lattice results; the SM prediction still allows NP contributions to $|M_{12}^s|$ of order 20% [80].

Within a 2HDM setup, the leading contribution to $B_q - \bar{B}_q$ $(q = d, s)$ mixing comes from the box diagrams shown in Fig. 7, where the G-boson is replaced by the charged Higgs H^+, and the fermions $u_{i,j}$ are replaced by (t, t'). Thus, the net contribution to the mass difference $\Delta M_q = 2|M_{12_q}|$ is given by [39]:

$$M_{12_q} = \frac{G_F^2}{12\pi^2} M_W^2 f_{B_q}^2 B_q M_{B_q} \left[M_{WW} + M_{HH} + M_{HW} \right], \tag{25}$$

where

$$
\begin{aligned}
M_{WW} &= \lambda_{bq}^{t\,2} \eta_{tt} S_{WW}(x_t) + \lambda_{bq}^{t'\,2} \eta_{t't'} S_{WW}(x_{t'}) + 2\,\lambda_{bq}^t \lambda_{bq}^{t'} \eta_{tt'} S_{WW}(x_t, x_{t'}), \\
M_{HH} &= \lambda_{bq}^{t\,2} S_{HH}(y_t) + \lambda_{bq}^{t'\,2} S_{HH}(y_{t'}) + 2\,\lambda_{bq}^t \lambda_{bq}^{t'} S_{HH}(y_t, y_{t'}), \\
M_{HW} &= \lambda_{bq}^{t\,2} S_{HW}(x_t, z) + \lambda_{bq}^{t'\,2} S_{HW}(x_{t'}, z) + 2\,\lambda_{bq}^t \lambda_{bq}^{t'} S_{HW}(x_t, x_{t'}, z),
\end{aligned}
\tag{26}
$$

and $z = \frac{m_{H^+}^2}{m_W^2}$, $x_i = \frac{m_i^2}{m_W^2}$, $y_i = \frac{m_i^2}{m_{H^+}^2}$ $(i = t$ or $t')$, $\lambda_{d_i d_j}^u \equiv V_{ud_i}^\star V_{ud_j}$. Here, M_{WW}, M_{HH} and M_{HW} are the contributions from the box diagrams with the combination of the gauge bosons (W, W), (W, H) and (H, H) in the internal lines (H stands for the charged Higgs), respectively. The detail expression for the various Inami-Lim functions $S_{i,j}$ are given in Ref. [39].

For the B-physics parameters we use the inputs given in Table I and for the 4th generation quark masses we take $m_{t'} = 500$ GeV and $m_{b'} = 450$ GeV.

$f_{bd}\sqrt{B_{bd}} = 0.224 \pm 0.015$ GeV [81, 82]	$\|V_{ub}\| = (32.8 \pm 2.6) \times 10^{-4}$ [a]
$\xi = 1.232 \pm 0.042$ [81, 82]	$\|V_{cb}\| = (40.86 \pm 1.0) \times 10^{-3}$
$\eta_t = 0.5765 \pm 0.0065$ [83]	$\gamma = (73.0 \pm 13.0)°$
$\Delta M_s = (17.77 \pm 0.12)ps^{-1}$	$\mathcal{BR}(B \to X_s\gamma) = (3.55 \pm 0.25) \times 10^{-4}$
$\Delta M_d = (0.507 \pm 0.005)ps^{-1}$	$m_b(m_b) = 4.23\, GeV$
$f_B = (0.208 \pm 0.008)$ GeV	$\alpha_s(M_Z) = 0.11$
$m_t^{pole} = (170 \pm 4)$ GeV	$\tau_{B+} = 1.63\, ps$
	$m_\tau = 1.77$ GeV

[a]It is the weighted average of $V_{ub}^{inc} = (40.1 \pm 2.7 \pm 4.0) \times 10^{-4}$ and $V_{ub}^{exc} = (29.7 \pm 3.1) \times 10^{-4}$ for the inclusive and exclusive values, respectively. In our numerical analysis, we increase the error on V_{ub} by 50% and take the total error to be around 12% due to the appreciable disagreement between the two determinations.

TABLE I: *Inputs used for the B-physics parameters in the analysis below. When not explicitly stated, we take the inputs from Particle Data Group [52].*
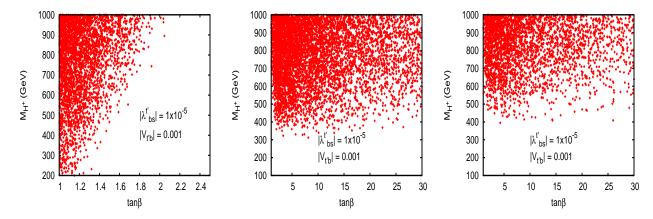

FIG. 8: *The "3+1" scenario, $V_{t'b} = 0.001$ ($\|\lambda_{sb}^{t'}\| = 10^{-5}$): the allowed parameter space in the $m_{H^+} - \tan\beta$ plane, following constraints from $B \to X_s\gamma$ and B_q-$\bar{B}_q$ mixing, in the 4G2HDMI (left), the 4G2HDMII (middle) and the 4G2HDMIII (right), for $m_{t'} = 500$ GeV, $m_{b'} = 450$ GeV, $\epsilon_b = m_b/m_{b'}$ and $\epsilon_t = 0.34(\sim m_t/m_{t'})$. Figure taken from [39].*

3. Constraints from b-Physics: results

For the "standard" 2HDMII with four generations we find that the constraints from $Br(B \to X_s\gamma)$ and ΔM_q ($q = d,s$) have a simple pattern in the $m_{H^+} - \tan\beta$ plane. In particular, with $m_{t'} \sim 500$ GeV we find that $M_{H^+} \gtrsim 600$ GeV for $\tan\beta = 1$, while $M_{H^+} \gtrsim 500$ GeV for $\tan\beta = 5$.

For the 4G2HDM's of types I, II and III, the combined constraints on their parameter space from both $Br(B \to X_s\gamma)$ and ΔM_q ($q = d,s$), are summarized below. In Figs. 8 and 9 we show a sample of the results obtained in [39], where the allowed ranges are shown in the $m_{H^+} - \tan\beta$ and the $\tan\beta - \epsilon_t$ planes, respectively. In these plots we use $\|V_{t'b}\| = 0.001$ - corresponding to the "3+1" scenario with a negligible 4th-3rd generation mixing, i.e., with $\|\lambda_{sb}^{t'}\| = 10^{-5}$ correspondingly. We see e.g., that in the 4G2HDMI, the "3+1" scenario typically imposes $\tan\beta \sim 1$ with ϵ_t typically larger than about 0.4 when $m_{H^+} \lesssim 500$ GeV. In the 4G2HDMII and the 4G2HDMIII one observes a similar correlation between $\tan\beta$ and m_{H^+}, however, larger $\tan\beta$ are allowed for $\epsilon_t \lesssim m_t/m_{t'}$ and a charged Higgs mass is typically heavier than 400 GeV.

For the case of a Cabbibo size mixing between the 4th and 3rd generation quarks, we set $\|V_{t'b}\| = \|V_{tb'}\| = 0.2$ and show in Figs. 10 and 11 the allowed parameter space in the $m_{H^+} - \tan\beta$ and $\tan\beta - \epsilon_t$ planes, in the 4G2HDM's of types I, II and III, with $m_{t'} = 500$ GeV, $m_{b'} = 450$ GeV and $\epsilon_b = m_b/m_{b'}$. In the 4G2HDMII and the 4G2HDMIII we see a similar behavior as in the no-mixing case (i.e., as in the case $V_{t'b} \to 0$), while in the 4G2HDMI we see that "turning on" $V_{t'b}$ allows for a slightly larger $\tan\beta$, i.e., up to $\tan\beta \sim 5$ for $\epsilon_t \gtrsim 0.9$. Also, similar to the no mixing case, larger values of $\tan\beta$ are allowed in the 4G2HDMII and 4G2HDMIII. Furthermore, $m_{H^+} \sim 300$ GeV and $\tan\beta \sim 1$ are allowed in the 4G2HDMI.
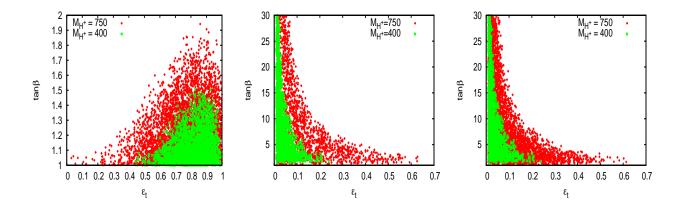
FIG. 9: *The "3+1" scenario, $V_{t'b} = 0.001$ ($|\lambda_{sb}^{t'}| = 10^{-5}$): the allowed parameter space in the $\tan\beta - \epsilon_t$ plane, following constraints from $B \to X_s\gamma$ and $B_q\text{-}\bar{B}_q$ mixing, in the 4G2HDMI (left), the 4G2HDMII (middle) and the 4G2HDMIII (right), for $m_{t'} = 500$ GeV, $m_{b'} = 450$ GeV, $\epsilon_b = m_b/m_{b'}$ and with $m_{H+} = 400$ and 750 GeV. Figure taken from [39].*
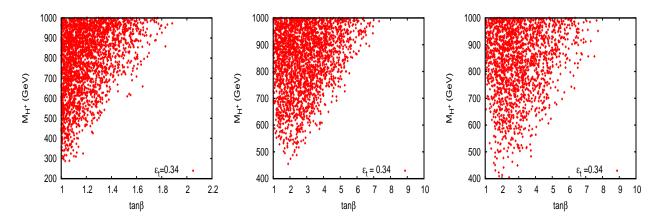

FIG. 10: *The Cabibbo size mixing case, $V_{t'b} = 0.2$ ($|\lambda_{sb}^{t'}| = 0.004$): the allowed parameter space in the $m_{H+} - \tan\beta$ plane, following constraints from $B \to X_s\gamma$ and $B_q\text{-}\bar{B}_q$ mixing, in the 4G2HDMI (left), 4G2HDMII (middle) and 4G2HDMIII (right), for $m_{t'} = 500$ GeV, $m_{b'} = 450$ GeV, $\epsilon_b = m_b/m_{b'}$ and $\epsilon_t = 0.34(\sim m_t/m_{t'})$. Figure taken from [39].*

D. Combined constraints and points of interest

In Table II we give a sample list of interesting points (models) in parameter space of the 4G2HDMI that "survive" all constraints from EWPD and flavor physics in the 4G2HDMI, for $m_h = 125$ GeV, $\tan\beta = 1$ and $\epsilon_t = m_t/m_{t'}$. The list includes (see also caption to Table II) models with a 4th generation mass splitting (between the up and down partners of both the 4th family quarks and leptons) larger than 150 GeV, models where both the 4th generation quarks and leptons are nearly degenerate, models with a light to intermediate neutral Higgs spectrum, i.e., $m_h = 125$ GeV and m_A or m_H in the range 150 GeV $-$ 300 GeV, models with a large inverted mass hierarchy in the quark doublet, i.e., $m_{b'} - m_{t'} > 150$ GeV, models with a light charged Higgs with a mass smaller than 400 GeV and models with a Cabibbo-size as well as an $\mathcal{O}(0.01)$ size $t' - b/t - b'$ mixing angle.
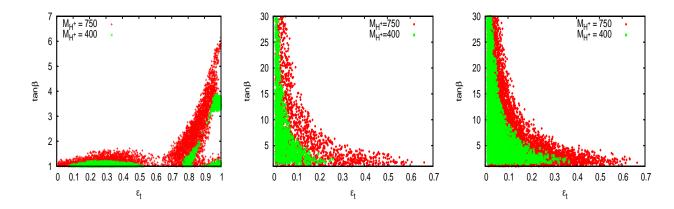
FIG. 11: *The Cabibbo size mixing case, $V_{t'b} = 0.2$ ($|\lambda_{sb}^{t'}| = 0.004$): the allowed parameter space in the $\tan\beta - \epsilon_t$ plane, following constraints from $B \to X_s\gamma$ and $B_q\text{-}\bar{B}_q$ mixing, in the 4G2HDMI (left), 4G2HDMII (middle) and 4G2HDMIII (right), for $m_{t'} = 500$ GeV, $m_{b'} = 450$ GeV, $\epsilon_b = m_b/m_{b'}$ and with $m_{H^+} = 400$ and 750 GeV. Figure taken from [39].*

	4G2HDMI: $m_h = 125$ GeV, $\tan\beta = 1$, $\epsilon_t = m_t/m_{t'}$									
Point #	$m_{t'}$	$m_{b'}$	$m_{\nu'}$	$m_{\tau'}$	m_A	m_H	m_{H^+}	$\sin\theta_{34}$	α	$\|\lambda_{sb}^{t'}\|$
1	570	403	118	184	319	993	806	0.02	0.46π	< 0.002
2	596	435	124	277	840	172	595	0.09	0.32π	< 0.0005
3	425	591	1151	1085	817	203	646	0.08	0.46π	< 0.001
4	441	595	385	556	180	998	661	0.21	0.69π	< 0.001
5	429	580	587	759	978	304	454	0.13	0.95π	< 0.0005
6	555	564	1185	1180	501	674	661	0.06	0.62π	< 0.0007
7	409	401	424	429	509	837	472	0.1	0.68π	< 0.0006
8	500	450	1079	1005	745	439	750	0.05	$\pi/2$	< 0.0006
9	500	450	160	176	733	414	750	0.05	$\pi/2$	< 0.0006
10	500	450	786	652	833	308	750	0.2	$\pi/2$	< 0.0006
11	500	450	211	268	798	289	750	0.2	$\pi/2$	< 0.0006
12	450	500	711	618	500	215	300	0.2	$\pi/2$	< 0.004
13^a	450	500	108	253	872	295	300	0.2	$\pi/2$	< 0.004

^{a}Points 12 and 13 require $\epsilon_b \lesssim m_b/m_{b'}$ in order to have $\text{BR}(b' \to tH^+) \sim \mathcal{O}(1)$ (see Fig. 17).

TABLE II: List of points (models) in parameter space for the 4G2HDM's of types I with $m_h = 125$ GeV, $\tan\beta = 1$ and $\epsilon_t = m_t/m_{t'}$, allowed at 95%CL by EWPD and B-physics flavor data. Points 1-2 have $m_{t'} - m_{b'} > 150$ GeV, while points 3-5 have a large inverted splitting $m_{b'} - m_{t'} > 150$ GeV. Points 6 and 7 have nearly degenerate 4th generation quark and lepton doublets. Points 8-11 give $\text{BR}(t' \to th) \sim \mathcal{O}(1)$ (see Fig. 16 in section V), while points 12 and 13 give $\text{BR}(b' \to tH^+) \sim \mathcal{O}(1)$ (see Fig. 17 in section V). Point 4 has a light 180 GeV pseudoscalar Higgs (A) and points 12 and 13 have a light 300 GeV charged Higgs. Points 1,8 and 9 have a small $t' - b/t - b'$ mixing angle ($\theta_{34} \le 0.05$), while points 4 and 10-13 have a Cabibbo-size $t' - b/t - b'$ mixing angle ($\theta_{34} \sim 0.2$).

IV.   OTHER USEFUL EFFECTS IN FLAVOR PHYSICS

We discuss below some important low energy observables which are potentially sensitive to the 4th generation dynamics within the multi-Higgs framework, and have shown some degree of discrepancy between their measured values and the SM predictions.

A.   Muon $(g-2)$ and lepton flavor violation

The muon anomalous magnetic moment (μAMM), $a_\mu = (g_\mu - 2)/2$, is well known to plays an important role in the search for NP. In the SM, the total contributions to the μAMM, a_μ^{SM}, can be divided into three parts: the QED, the electroweak (EW) and the hadronic contributions. While the QED [84] and EW [85] contributions are well understood, the main theoretical uncertainty lies with the hadronic part which is difficult to control [86].

Since the first precision measurement of a_μ, there has been a discrepancy between its experimental value and the SM prediction. This discrepancy has been slowly growing due to recent impressive theoretical and experimental progress. Comparing theory and experiment, the deviation amounts to [87]:

$$a_\mu^{exp} - a_\mu^{SM} = (255 \pm 80) \cdot 10^{-11} \qquad (27)$$

which corresponds to a $\sim 3\sigma$ effect. In order to confirm this result the uncertainties have to be further reduced.

It is interesting to interpret the difference as a contribution from loop exchanges of new particles. A number of groups have studied the contribution to a_μ in various extensions of the SM to constrain their parameters space (for reviews see Ref. [88]). In most extensions of the SM, new charged or neutral states can contribute to the μAMM at the one-loop (lowest) level. In Ref. [89], we have shown that the $\sim 3\sigma$ excess in a_μ (with respect to the SM prediction) can be accounted for by one-loop exchanges of the heavy 4th generation neutrino (ν') in the 4G2HDMI setup when applied to the leptonic sector (i.e., where the "heavy" Higgs doublet couples only to the 4th generation lepton doublet and the "light" Higgs doublet couples to leptons of the lighter 1st-3rd generations, see [89]).
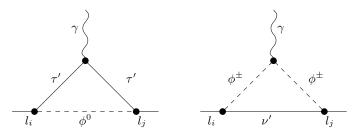

FIG. 12: *One-loop diagrams for $l_i \to l_j\gamma$ with charged and neutral scalar exchanges.*

The effective vertex of a photon with a charged fermion can in general be written as

$$\bar{u}(p')e\Gamma_\mu u(p) = \bar{u}(p')e\left[\gamma_\mu F_1(q^2) + \frac{i\sigma_{\mu\nu}q^\nu}{2m_f}F_2(q^2)\right]u(p)\,, \qquad (28)$$

where, to lowest order, $F_1(0) = 1$ and $F_2(0) = 0$. While $F_1(0)$ remains unity at all orders due to charge conservation, quantum corrections yield $F_2(0) \neq 0$. Thus, since $g_\mu \equiv 2 \cdot (F_1(0) + F_2(0))$, it follows that $a_\mu \equiv (g_\mu - 2)/2 = F_2(0)$.

In the 4G2HDMI [39, 89] the one-loop contribution to the muon anomaly can be subdivided as

$$a_\mu = [a_\mu]_W^{SM4} + [a_\mu]_\mathcal{H}^{4G2HDMI}\,, \qquad (29)$$

where $[a_\mu]_\mathcal{H}^{4G2HDMI}$ contains the charged and neutral Higgs contributions coming from the one-loop diagrams in Fig. 12, where the diagrams with τ' and ν' in the loop dominate. The SM4-like contribution, $[a_\mu]_W^{SM4}$, comes from the one-loop diagram with $W^\pm - \nu'$ in the loop and is given by [90]:

$$\frac{[a_\mu]_W^{SM4}}{|U_{24}|^2} = \frac{G_F m_\mu^2}{4\sqrt{2}\pi^2}A(x_{\nu'})\,, \qquad (30)$$

where U_{24} is the 24 element of the CKM-like PMNS leptonic matrix, $x_i = m_i^2/m_W^2$. For values of $m_{\nu'}$ in the range 100 GeV $\lesssim m_{\nu'} \lesssim 1000$ GeV, one finds $1.5 \times 10^{-9} \lesssim [a_\mu]_W^{SM4}/|U_{24}|^2 \lesssim 3.0 \times 10^{-9}$, so that for $|U_{24}|^2 << 1$ (as expected) the simple SM4 cannot accommodate the observed discrepancy in a_μ. The detail expression for $[a_\mu]_\mathcal{H}^{4G2HDMI}$ has been given in [89]. It is interesting to note that the dominant contribution to $[a_\mu]_\mathcal{H}^{4G2HDMI}$, or for that matter to a_μ, comes from the charged Higgs loops and the contribution from diagrams with the neutral Higgs exchanges are subleading [89]. In addition, a_μ was found to be sensitive only to the product $\delta_{\Sigma_2} \cdot \delta_{U_2}$, where

$$\delta_{U_i} \equiv \frac{U_{i4}^*}{U_{44}^*}\,,\ \delta_{\Sigma_i} \equiv \frac{\Sigma_{4i}^{e*}}{\Sigma_{44}^\nu}\,, \qquad (31)$$

and $\Sigma^e(\Sigma^\nu)$ are the new mixing matrices (i.e., in the 4G2HDMI) in the charged(neutral)-leptonic sectors. That is, similar to the quark sector (see Eq. 12), these matrices are obtained after diagonalizing the lepton mass matrices

$$\Sigma_{ij}^e = L_{R,4i}^\star L_{R,4j}\,,\ \Sigma_{ij}^\nu = N_{R,4i}^\star N_{R,4j}\,, \qquad (32)$$

where L_R, N_R are the rotation (unitary) matrices of the right-handed charged and neutral leptons, respectively.[3]

In Fig. 13 we plot a_μ as a function of the product $\delta_{\Sigma_2} \cdot \delta_{U_2}$ (assuming its real) for several values of $m_{\nu'}$ and m_{H^+} and fixing $m_{\tau'} = m_{\nu'}$. Depending on the mass $m_{\nu'}$, we find that $\delta_{U_2} \cdot \delta_{\Sigma_2} \sim 10^{-3} - 10^{-2}$ is typically required to accommodate the measured value of a_μ.
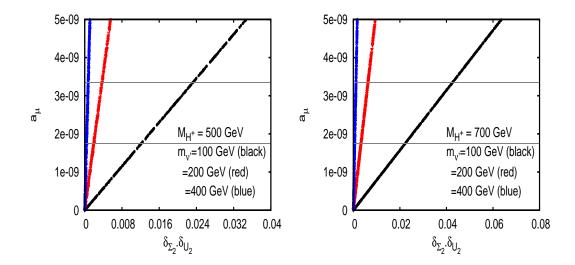

FIG. 13: *The muon $g-2$ as a function of the product $\delta_{\Sigma_2} \cdot \delta_{U_2}$, for $m_{\nu'} = 100$, 200, 400 GeV, $m_{\tau'} = m_{\nu'}$ and with $m_{H^+} = 500$ GeV (left) and $m_{H^+} = 700$ GeV (right). The horizontal lines are the measured 1-σ bounds on a_μ (see Eq. 27). Figure taken from [89].*

The constraint on the 4G2HDMI parameters and in particular on the quantities δ_{Σ_2} and δ_{U_2} which control the μAMM were studied in [89], by analyzing the lepton flavor violating (LFV) decays $\tau \to \mu\gamma$ and $\mu \to e\gamma$. These decays are absent in the SM, and are useful for constraining NP models that can potentially contribute to the muon anomaly.

The current experimental 90%CL upper bounds on these LFV decays are [52, 91]

$$Br(\tau \to \mu\gamma) < 4.4 \times 10^{-8} \quad , \quad Br(\mu \to e\gamma) < 2.4 \times 10^{-12} \ . \tag{33}$$

The amplitude for the transition $\ell_i \to \ell_j\gamma$ can be defined as

$$\mathcal{M}(\ell_i \to \ell_j\gamma) = \bar{u}_{\ell_j}(p') \left[i\sigma_{\mu\nu}q^\nu \left(A + B\gamma_5 \right) \right] u_{\ell_i}(p)\epsilon^{\mu*} \ , \tag{34}$$

where $\epsilon^{\mu*}$ is the photon polarization. The decay width is then given by

$$\Gamma(\ell_i \to \ell_j\gamma) = \frac{m_{\ell_i}^3}{8\pi} \left(1 - \frac{m_{\ell_j}^2}{m_{\ell_i}^2} \right) \left[\left(1 + \frac{m_{\ell_j}^2}{m_{\ell_i}^2} \right) \left(|A|^2 + |B|^2 \right) + 4\frac{m_{\ell_j}}{m_{\ell_i}} \left(|A|^2 - |B|^2 \right) \right] \ . \tag{35}$$

Here also, the new 4G2HDMI contribution to the amplitude, $\mathcal{M}(\ell_i \to \ell_j\gamma)^{4G2HDMI}$, can be divided as

$$\mathcal{M}(\ell_i \to \ell_j\gamma)^{4G2HDMI} \equiv \mathcal{M}_W^{SM4}(\ell_i \to \ell_j\gamma) + \mathcal{M}_{H^+}^{4G2HDMI}(\ell_i \to \ell_j\gamma) + \mathcal{M}_{\mathcal{H}^0}^{4G2HDMI}(\ell_i \to \ell_j\gamma) \ , \tag{36}$$

where $\mathcal{M}_W^{SM4}(\ell_i \to \ell_j\gamma)$ is the SM4-like W-exchange contribution which is much smaller than the charged and neutral Higgs amplitudes, $\mathcal{M}_{H^+}^{4G2HDMI}(\ell_i \to \ell_j\gamma)$ and $\mathcal{M}_{\mathcal{H}^0}^{4G2HDMI}(\ell_i \to \ell_j\gamma)$ (calculated from the diagrams in Fig. 12). As in the μAMM case, the dominant contribution to LFV decays was found the be from the charged Higgs exchange diagrams [89]. In addition, the decays $\mu \to e\gamma$ and $\tau \to \mu\gamma$ are sensitive to δ_{U_2} and δ_{Σ_2} through the products $(\delta_{U_2}\delta_{\Sigma_1}, \delta_{U_1}\delta_{\Sigma_2})$ and $(\delta_{U_3}\delta_{\Sigma_2}, \delta_{U_2}\delta_{\Sigma_3})$, respectively, so that, in principle, one can avoid constraints on the quantities δ_{U_2} and δ_{Σ_2} if $\delta_{U_1}, \delta_{U_3}, \delta_{\Sigma_1}$ and δ_{Σ_3} are sufficiently small.

---

[3] Note that since $N_{R,4i}$ and $L_{R,4j}$ parameterize mixings among the 4th generation and the 1st-3rd generations leptons, one expects $\Sigma_{ij}^\ell \ll \Sigma_{4k}^\ell$ for $i, j, k = 1, 2, 3$, see Eq. 32.
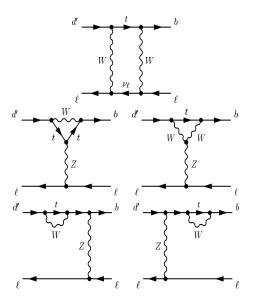
FIG. 14: *Dominant SM diagrams for the decay $B_{d'} \to \ell^+\ell^-$, $d' = d$ or s.*

In Ref. [89], we have shown that it is possible to address both the $BR(\mu \to e\gamma)$ and the muon anomaly a_μ within the 4G2HDMI framework, if $\delta_{U_1} \ll \delta_{U_2}$ and $\delta_{\Sigma_1} \ll \delta_{\Sigma_2}$, which is indeed expected if we consider the observed hierarchical pattern of the quark's CKM matrix as a guide. However, in order to account also for the measured upper limit on $BR(\tau \to \mu\gamma)$ (see Eq. 33), one requires $\delta_{U_3} < \delta_{U_2}$ and $\delta_{\Sigma_3} < \delta_{\Sigma_2}$. Therefore, the typical benchmark texture for the 4th generation elements of the matrices U_{i4} Σ_{4i}^e that can account for the observed muon anomaly and still be consistent with the current constraints from the LFV decays $\tau \to \mu\gamma$ and $\mu \to e\gamma$ is

$$U_{i4} \sim (\Sigma_{4i}^e)^T \simeq \begin{pmatrix} \epsilon^5 \\ \epsilon \\ \epsilon^2 \\ 1 \end{pmatrix} , \tag{37}$$

where e.g., $\epsilon \sim 0.1$ for $m_{\nu'} = 100$ GeV.

The above texture implies a hierarchical pattern which is different than one would expect from the observed hierarchical pattern of the quark's CKM matrix. Nonetheless, without a fundamental theory of flavor, our insight for flavor should be data driven also in the leptonic sector. Besides, the above texture is sensitive to the current precision in the measurement of the muon g-2 which can change e.g., if more accurate calculations end up showing that part of the hadronic contributions cannot be ignored.

B. Insight from B physics

1. $B_s \to \mu^+\mu^-$

Among the various B_q rare decays, the purely leptonic $B_{d/s} \to \mu^+\mu^-$ decays are highly sensitive to indirect effects of NP, since the quark level decays are based on the FCNC $b \to d, s$ transitions which are severely (loop) suppressed in the SM. In particular, the decay $B_s \to \mu^+\mu^-$ has received special attention in the past decade, since its branching fraction, $Br(B_s \to \mu^+\mu^-)$, can be significantly enhanced by loop exchanges of new particles predicted by various NP scenarios. For example, $Br(B_s \to \mu^+\mu^-)$ imposes restrictive constraints on the SUSY parameter space (see e.g.,

[92, 95]), where in some scenarios better limits than those obtained from direct searches have been claimed. However, the excluded SUSY parameter space depends strongly on the choice of $\tan\beta$ since the $B_s \to \mu^+\mu^-$ rate typically varies as $(\tan\beta)^6$.
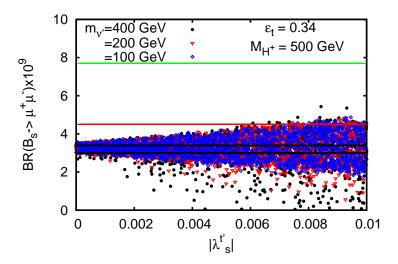

FIG. 15: $BR(B_s \to \mu\mu)$ as a function of $\lambda_{bs}^{t'} \equiv V_{t'b}V_{t's}^*$, from box diagrams with H^+ and (t,ν'), (t',ν') exchanges in the 4G2HDMI. The parameters δ_{U_2} and δ_{Σ_2} are varied within the constraints imposed by a_μ (see previous section), keeping both of them $\lesssim 0.2$. Also shown are the experimental 95% CL upper bounds from LHCb (red horizontal line) and from CMS (green horizontal line). The SM predicted range of values (at 1σ) is shown within the black horizontal lines. Figure taken from [89].

In the LHC era the current limit on $Br(B_s \to \mu^+\mu^-)$ has been improved. The two different experiments LHCb and CMS, using $1fb^{-1}$ and $5fb^{-1}$ data sample, respectively, yield [93, 94]

$$Br(B_s \to \mu^+\mu^-) < 4.5 \times 10^{-9} , \qquad LHCb@95\%CL$$
$$< 7.7 \times 10^{-9} , \qquad CMS@95\%C \qquad (38)$$

whereas the SM prediction for this decay is [12]:

$$Br(B_s \to \mu^+\mu^-) = (3.2 \pm 0.2) \cdot 10^{-9} . \qquad (39)$$

In fact, LHCb has the sensitivity to measure the $Br(B_s \to \mu^+\mu^-)$ down to $\sim 2 \times 10^{-9}$, which is about 5σ smaller than the SM prediction.

In general, the matrix element for the decay $\bar{B}_s \to \ell^+\ell^-$ can be written as [96]

$$\mathcal{M} = \frac{G_F\alpha}{2\sqrt{2}\pi\sin\theta_W^2} \left[F_S\,\bar{\ell}\ell + F_P\,\bar{\ell}\gamma_5\ell + F_A\,P^\mu\bar{\ell}\gamma_\mu\gamma_5\ell\right] , \qquad (40)$$

where P^μ is the four momentum of the initial B_s meson and F_i's are functions of Lorentz invariant quantities. Squaring the matrix and summing over the lepton spins, we obtain the branching fraction

$$Br(\bar{B}_s \to \ell^+\ell^-) = \frac{G_F^2\alpha^2 M_{B_s}\tau_{B_s}}{64\pi^3}\sqrt{1 - \frac{4m_\ell^2}{M_{B_s}^2}}\left[\left(1 - \frac{4m_\ell^2}{M_{B_s}^2}\right)|F_S|^2 + |F_P + 2m_\ell F_A|^2\right] . \qquad (41)$$

In the SM, the dominant effect in $\bar{B}_s \to \ell^+\ell^-$ arise from the diagrams shown in Fig. 14, which contribute only to F_A in Eq. 40.

As in other NP models, in the 4G2HDMI there will be contributions to F_S, F_P and F_A coming from the charged-Higgs exchange penguin and box diagrams (replacing $W^+ \to H^+$ in Fig. 14). In Ref. [39], constraint on the 4G2HDMI parameter spaces were estimated, using the recent data on $Br(B_s \to \mu^+\mu^-)$. This was done in the context of the muon $(g-2)$, in the sense that only those interactions (in the leptonic vertex) which are associated with a_μ have been considered. In particular, considering only the $\ell^\pm\nu'H^\pm$ vertex, the only diagrams that contribute to $\bar{B}_s \to \ell^+\ell^-$

are the Higgs-exchange box diagrams in Fig. 14, where one or two W-bosons are replaced by H^+ and (t, ν_ℓ) are being replaced by both (t, ν') and (t', ν'). It was then found that the contribution from the new box diagrams in the 4G2HDMI that involve the heavy 4th generation neutrino is consistent with the current experimental bound on $BR(B_s \to \mu\mu)$ for values of δ_{U_2} and δ_{Σ_2} that reproduce the observed muon $g - 2$, see Fig. 15.

It is also interesting to note that the $\text{Br}(B_s \to \mu^+\mu^-)$, in both the SM4 and the 4G2HDMI, can differ from the SM value by at-most a factor of O(3) in either direction (for a detail discussions see [89]).

2. $B^+ \to \tau^+\nu$ and $B \to D^{(*)}\tau\nu$

Other purely leptonic and semileptonic decays of the B meson, such as $B \to \tau$ decays, can also provide useful tests of the SM and its extensions. Of particular interest are the purely leptonic $B \to \tau\nu$ and the semileptonic $B^+ \to D^{(*)}\tau\nu$ decays. The SM contribution to the branching ratios of these decays arise at the tree-level from the charged weak interactions. An important NP contribution to these decays is the tree-level exchange of a charged Higgs in multi-Higgs models, so that these decays offer interesting probes of the Higgs sector and, particularly, of its Yukawa interactions.

The SM expression for the decay rate of $B \to \tau\nu$ is given by

$$Br(B \to \tau\nu)_{SM} = \frac{G_F^2 m_\tau^2 m_B}{8\pi} (1 - \frac{m_{\tau^2}}{m_B^2})^2 f_B^2 |V_{ub}|^2 \tau_B. \tag{42}$$

where f_B is the decay constant and τ_B is the B^+ life time. The SM prediction for $Br(B^+ \to \tau^+\nu)$ is, therefore, sensitive to the decay constant f_B and to the CKM element $|V_{ub}|$ and is thus limited by the uncertainty in the determination of these quantities. Using the available constraints on f_B and the inclusive determination of V_{ub}: $f_B = 200 \pm 20$ MeV and $V_{ub} = (39.9 \pm 1.5 \pm 4.0) \cdot 10^{-4}$ [97], the SM prediction for the decay rate is

$$Br(B \to \tau\nu)_{SM} = (0.86 \pm 0.12) \cdot 10^{-4} . \tag{43}$$

Furthermore, the SM prediction on $\text{Br}(B \to \tau\nu)$, obtained directly from a fit to various other observables (i.e., without using V_{ub} and the lattice results for f_B) is [97]

$$Br(B \to \tau\nu)_{SM} = (0.73 \pm 0.12) \cdot 10^{-4} . \tag{44}$$

Both results show some degree of discrepancy with the current world average on $BR(B \to \tau\nu)$ which is [79],

$$Br(B^+ \to \tau^+\nu_\tau) = (1.67 \pm 0.3) \cdot 10^{-4}. \tag{45}$$

We want to indicate here how the 4G2HDM can address this if the discrepancy is confirmed.

From the theoretical point of view, several models of NP predict large deviations from the SM for processes involving third generation fermions. For instance, in a "standard" 2HDM where the two Higgs doublets are coupled separately to up- and down- type quarks (i.e., the 2HDMII setup described in section II), the $B \to \tau\nu$ amplitude receives an additional tree-level contribution from the heavy charged-Higgs exchange, leading to

$$\frac{Br(B \to \tau\nu)^{2HDMII}}{Br(B \to \tau\nu)^{SM}} = \left[1 - \frac{m_B^2 \tan^2\beta}{M_H^2}\right] , \tag{46}$$

so that for large $\tan\beta$, the r.h.s of Eq. 46 can be significantly different from "1". However, in this particular case (of the 2HDMII), the charged-Higgs contribution reduces the SM value for the branching ratio, thus further worsening the situation with respect to the experimentally measured value.

In the 4G2HDMI, the effective tree-level interactions that will contribute to $B \to \tau\nu$ can be written as

$$\begin{aligned} \mathcal{H}_{eff} &= \frac{G_F V_{ub}}{\sqrt{2}} \left[\bar{u}\gamma_\mu(1 - \gamma_5)b\,\bar{\tau}\gamma^\mu(1 - \gamma_5)\nu - \frac{m_\tau m_b A_{bu}}{M_H^2} \left\{ A_u^\ell \bar{u}(1 + \gamma_5)b\,\bar{\tau}(1 - \gamma_5)\nu \right. \right. \\ &\left. \left. + A_d^\ell \bar{u}(1 + \gamma_5)b\,\bar{\tau}(1 + \gamma_5)\nu \right\} \right] , \end{aligned} \tag{47}$$

where the second term represents the tree-level charged-Higgs exchange and the first term results from the diagram with W-boson exchange. Also, A_{bu}, A_u^ℓ and A_d^ℓ are factors coming from the $b \to uH$ and $\tau \to \nu_\tau H$ vertices,

respectively, given by

$$
\begin{aligned}
A_{bu} &= \tan\beta - (\tan\beta + \cot\beta)(\Sigma_{bb} + \frac{m_{b'}}{m_b}\frac{V_{ub'}}{V_{ub}}\Sigma_{b'b}), \\
A_u^\ell &= -\tan\beta + (\tan\beta + \cot\beta)\left\{\Sigma_{33}^\ell U_{33} + \frac{m_{\tau'}}{m_\tau}\Sigma_{43}^\ell U_{43}\right\}, \\
A_d^\ell &= -\frac{m_{\nu_{\tau'}}}{m_\tau}(\tan\beta + \cot\beta)\Sigma_{43}^\nu U_{34}.
\end{aligned}
\tag{48}
$$

A simple calculation, using Eqs. 47 and 48, yields

$$
Br(B \to \tau\nu) = Br(B \to \tau\nu)_{SM}\left[\left|1 - \frac{m_B^2}{M_H^2}A_{bu}A_u^\ell\right|^2 + \left|\frac{m_B^2}{M_H^2}A_{bu}A_d^\ell\right|^2\right].
\tag{49}
$$

Thus, taking for example $\Sigma_{ij} \approx m_j/m_i$, only a moderate enhancement to $BR(B \to \tau\nu)$ is possible at large $\tan\beta$. If, on the other hand, $\Sigma_{ij} \gg m_j/m_i$, then the BR($B \to \tau\nu$) can be significantly enhanced compared to the SM prediction. Of course, the experimental deviations at the moment are only a few sigmas, but, if they get confirmed, then we have indicated here how we may be able to address them.

Semileptonic B decays such as $B \to D^{(*)}\tau\nu$ are more complicated to handle than the pure leptonic ones, since the theoretical predictions for these decays to exclusive final states require knowledge of the form factors involved. There are, however, several other observables (besides the branching fraction), such as the decay distributions and the τ polarization, which can be useful in this cases for probing NP.

As in the case of $B \to \tau\nu$, the semileptonic decay $B \to D^{(*)}\tau\nu$ is also known to be the a sensitive mode to the tree-level charged-Higgs exchange. Furthermore, the precise measurement of $B \to D^{(*)}\ell\nu$ at the B-factories and the theoretical developments of heavy-quark effective theory (HQET) has improved our understanding of exclusive semileptonic decays [52, 98].

In particular, the ratios $R(D^{(*)}) \equiv \mathrm{BR}(B \to D^{(*)}\tau\nu)/\mathrm{BR}(B \to D^{(*)}\ell\nu)$ reduces considerably the main theoretical uncertainties, hence, turns out to be a more useful observable [99]. The updated SM predictions of these rates, averaged over electron and muons, are given by [100],

$$
R(D)_{SM} = 0.297 \pm 0.017, \qquad\qquad R(D^*)_{SM} = 0.252 \pm 0.003,
\tag{50}
$$

so that at this level of precision the experimental uncertainties are expected to dominate.

The most recently measured values of these observables are given by [100],

$$
R(D)_{exp} = 0.440 \pm 0.058 \pm 0.042, \qquad\qquad R(D^*)_{exp} = 0.332 \pm 0.024 \pm 0.018 .
\tag{51}
$$

The measured values, therefore, exceed the SM predictions for $R(D)_{SM}$ and $R(D^*)_{SM}$ by 2.0σ and 2.7σ, respectively, so it is argued that the possibility of both the measured values agreeing with the SM is excluded at the 3.4σ level. In addition, the combined analysis of $R(D)$ and $R(D^*)$ rules out the 2HDMII charged Higgs boson with 99.8% confidence level for any value of $\tan\beta/M_H$ when combined with $\mathrm{Br}(B \to X_s\gamma)$, see [100]. Once again, it is not clear to us how serious to take the indications of the deviations in Eq. 51. Nonetheless, we briefly indicate here how this discrepancy (if experimentally confirmed) can be addressed in the 4G2HDMI, for which the effective tree-level interactions that contribute to $B \to D^{(*)}\tau\nu$ are given in Eq. 47 with the u-quark replaced by the c quark. Thus, similar to the case of $B \to \tau\nu$, we expect a moderate enhancement to both $R(D)$ and $R(D^*)$ in the 4G2HDMI if $\Sigma_{ij} \approx m_j/m_i$, and a larger effect for larger values of Σ_{ij}.

V. NEW ASPECTS OF THE PHENOMENOLOGY OF THE 4G2HDMI

In the 4G2HDMI (i.e., the 4G2HDM with $\beta_d = \beta_u = 0$, see Eq. 5) one obtains (see Eq. 13):

$$
\Sigma^d \simeq \begin{pmatrix} 0 & 0 & 0 & 0 \\ 0 & 0 & 0 & 0 \\ 0 & 0 & |\epsilon_b|^2 & \epsilon_b^\star \\ 0 & 0 & \epsilon_b & \left(1 - \frac{|\epsilon_b|^2}{2}\right) \end{pmatrix} , \;
\Sigma^u \simeq \begin{pmatrix} 0 & 0 & 0 & 0 \\ 0 & 0 & 0 & 0 \\ 0 & 0 & |\epsilon_t|^2 & \epsilon_t^\star \\ 0 & 0 & \epsilon_t & \left(1 - \frac{|\epsilon_t|^2}{2}\right) \end{pmatrix} ,
\tag{52}
$$

which leads to new interesting patterns (in flavor space) in the both the neutral and charged Higgs sectors. For example, the $\mathcal{H}^0 q_i q_j$ Yukawa interactions of Eqs. 8-11 ($\mathcal{H}^0 = h, H, A$), give rise to potentially enhanced tree-level
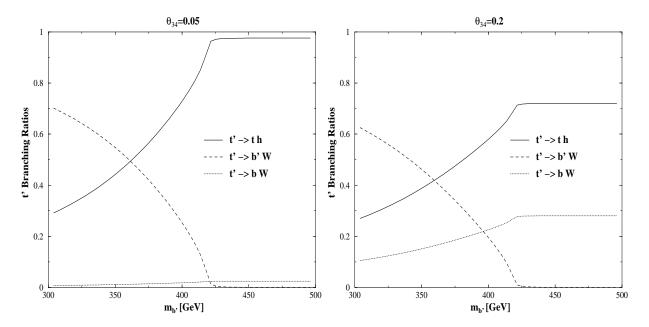
FIG. 16: *The branching ratios for the t' decay channels $t' \to th$, $t' \to bW$ and $t' \to b'W^{(\star)}$ ($W^{(\star)}$ is either on-shell or off-shell depending on the b' mass) in the 4G2HDMI, as a function of $m_{b'}$, for $m_h = 125$ GeV, $m_{t'} = 500$ GeV, $\epsilon_t = m_t/m_{t'}$, $\tan\beta = 1$, $\theta_{34} = 0.05$ (left) and $\theta_{34} = 0.2$ (right). Also, $\alpha = \pi/2$ and $m_{H^+} > m_{t'}$, $m_A > m_{t'}$ is assumed.*

$t' \to t$ and $b' \to b$ FC transitions, and absence of "dangerous" tree-level FCNC transitions between the 4th and the 1st and 2nd generations quarks as well as among the 1st-2nd and 3rd generation quarks. In particular, the FC $\mathcal{H}'t't$ interactions in this case are (taking $\alpha \to \pi/2$):

$$\mathcal{L}(ht't) = -\frac{g}{2}\frac{m_{t'}}{m_W}\epsilon_t\sqrt{1 + t_\beta^2}\ \bar{t}'\left(R + \frac{m_t}{m_{t'}}L\right)th \ , \tag{53}$$

$$\mathcal{L}(Ht't) = -\frac{g}{2}\frac{m_{t'}}{m_W}\epsilon_t\frac{\sqrt{1 + t_\beta^2}}{t_\beta}\ \bar{t}'\left(R + \frac{m_t}{m_{t'}}L\right)tH \ , \tag{54}$$

$$\mathcal{L}(At't) = i\frac{g}{2}\frac{m_{t'}}{m_W}\epsilon_t\frac{1 + t_\beta^2}{t_\beta}\ \bar{t}'\left(R - \frac{m_t}{m_{t'}}L\right)tA \ , \tag{55}$$

and similarly for the $\mathcal{H}^0 b'b$ vertices by changing $\epsilon_t \to \epsilon_b$ (and an extra minus sign in the $Ab'b$ coupling).

If $\epsilon_t \sim m_t/m_{t'}$, then the above $\mathcal{H}'t't$ couplings can become sizable, to the level that it might dominate the decay pattern of the t' (see below). In fact, large FC effects are also expected in $b' \to b$ transitions since, even for a very small $\epsilon_b \sim m_b/m_{b'}$, the FC $hb'b$ and $Ab'b$ Yukawa couplings can become sizable if e.g., $\tan\beta \sim 5$ for which case they are $\propto \frac{5m_b}{m_W}$. Therefore, such new FCNC $t' \to t$ and $b' \to b$ transitions can have drastic phenomenological consequences for high-energy collider searches of the 4th generation fermions, as we be discussed below.

Furthermore, the flavor diagonal interactions of the Higgs species with the up-quarks of the 1st, 2nd and 3rd generations are proportional to $\tan\beta$ in this model, thus being a factor of $\tan^2\beta$ larger than the corresponding "conventional" 2HDMII (i.e., the type II 2HDM) couplings (which are $\propto \cot\beta$). For example, this gives rise to an enhanced flavor diagonal $ht\bar{t}$ interactions, while suppressing the $ht'\bar{t}'$ one,

$$\mathcal{L}(htt) \approx \frac{g}{2}\frac{m_t}{m_W}\sqrt{1 + t_\beta^2}\left(1 - |\epsilon_t|^2\right)\ \bar{t}th \overset{|\epsilon_t|^2 \ll 1}{\longrightarrow} \frac{g}{2}\frac{m_t}{m_W}\sqrt{1 + t_\beta^2}\ \bar{t}th \ , \tag{56}$$

$$\mathcal{L}(ht't') \approx \frac{g}{4}\frac{m_{t'}}{m_W}\sqrt{1 + t_\beta^2}|\epsilon_t|^2\ \bar{t}'t'h \ , \tag{57}$$

when $|\epsilon_t|^2 \to 0$.

Another important new feature of this model occurs in the charged Higgs couplings involving the 3rd and 4th generation quarks, which are completely altered by the presence of the Σ_d and Σ_u matrices and can thus lead to
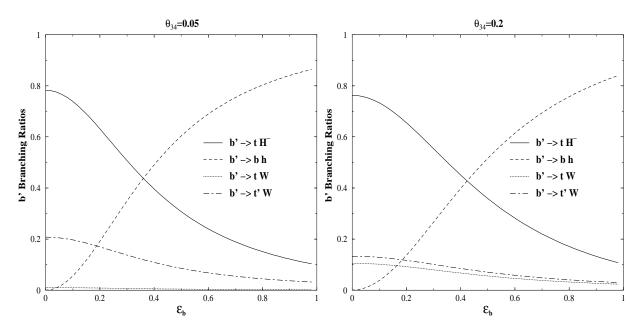
FIG. 17: *The branching ratios for the b' decay channels $b' \to tH^+$, $b' \to bh$, $b' \to tW$ and $b' \to t'W$ in the 4G2HDMI, as a function of ϵ_b for $m_h = 125$ GeV, $m_{b'} = 500$ GeV, $m_{t'} = 400$ GeV, $m_{H^+} = 300$ GeV, $\tan\beta = 1$, $\epsilon_t = m_t/m_{t'}$ and , $\theta_{34} = 0.05$ (left) and $\theta_{34} = 0.2$ (right). Also, $\alpha = \pi/2$ and $m_A > m_{b'}$ is assumed.*

interesting new effects in both the leptonic (see previous section) and quark sectors. For example, taking $V_{t'b}, V_{tb'} \ll V_{tb}, V_{t'b'}$, the $H^+t'b$ and H^+tb' Yukawa couplings are given in the 4G2HDMI by:

$$\mathcal{L}(H^+t'b) \approx \frac{g}{\sqrt{2}m_W} t_\beta \left(1 + t_\beta^{-2}\right) \bar{t}' \left(m_t \epsilon_t V_{tb} L - m_{b'} \epsilon_b V_{t'b'} R\right) b H^+ \ , \tag{58}$$

$$\mathcal{L}(H^+tb') \approx \frac{g}{\sqrt{2}m_W} t_\beta \left(1 + t_\beta^{-2}\right) \bar{t} \left(m_t' \epsilon_t^\star V_{t'b'} L - m_b \epsilon_b^\star V_{tb} R\right) b' H^+ \ . \tag{59}$$

Recalling that in the "standard" 2HDMII (which would underly a supersymmetric four generation model) the $\bar{t}_R b'_L H^+$ would be $\propto m_t V_{tb'}/t_\beta$, we find that in the 4G2HDMI the $\bar{t}_R b'_L H^+$ coupling is potentially enhanced by a factor of:

$$\frac{\bar{t}_R b'_L H^+ (\text{4G2HDMI})}{\bar{t}_R b'_L H^+ (\text{2HDMII})} \sim \epsilon_t \cdot t_\beta^2 \cdot \frac{m_t'}{m_t} \cdot \frac{V_{tb}}{V_{tb'}} \ , \tag{60}$$

so that if e.g., $t_\beta \sim 1$, and $\epsilon_t \sim m_t/m_{t'}$, there is a factor of $V_{tb}/V_{t'b}$ enhancement to the $\bar{t}_R b'_L H^+$ interaction.

These new aspects of phenomenology in the Yukawa interactions sector can have far reaching implications for collider searches of the heavy 4th generation quarks and leptons, as will be discussed in more detail in the next sections. To see that, one can study the new decay patterns of t' and b' that follow from the above new Yukawa terms. In particular, in Fig. 16 we plot the branching ratios of the leading t' decay channels (assuming $m_{H^+}, m_A > m_{t'}$): $t' \to th$, bW, $b'W^{(\star)}$ [$W^{(\star)}$ stands for either on-shell or off-shell W depending on $m_{b'}$], as a function of the b' mass. We use $m_h = 125$ GeV, $m_{t'} = 500$ GeV, $\tan\beta = 1$, $\epsilon_t = m_t/m_{t'}$ and $\theta_{34} = 0.05$ and 0.2. We see that the $BR(t' \to th)$ can easily reach $\mathcal{O}(1)$ (even for a rather large $\theta_{34} \sim 0.2$ for which $t' \to bW$ becomes sizable), in particular when $m_{t'} - m_{b'} < m_W$; see e.g., points 8-11 in Table II for which $BR(t' \to th) \sim \mathcal{O}(1)$.

In Fig. 17 we plot the branching ratios of the leading b' decay channels $b' \to tH^-$, bh, tW, $t'W$, as a function of ϵ_b for $m_{b'} = 500$ GeV, $m_h = 125$ GeV, $\tan\beta = 1$, $m_{H^+} = 300$ GeV, $\epsilon_t = m_t/m_{t'}$ and $\theta_{34} = 0.05$ and 0.2. We see that in the b' case the dominance of $b' \to tH^-$ (if kinematically allowed) should be much more pronounced due to the expected smallness of the $b - b'$ mixing parameter, ϵ_b, which controls the FC decay $b' \to bh$; see e.g., points 12 and 13 in Table II for which $BR(b' \to bH^-) \sim \mathcal{O}(1)$. On the other hand, if ϵ_b is larger than about 0.4, then $b' \to bh$ dominates.

VI. IMPLICATIONS OF THE 4G2HDMI FOR DIRECT SEARCHES OF 4TH GENERATION QUARKS

The direct searches of the 4th generation quarks at the LHC currently provide the most stringent limits on their masses. In particular, CMS reported a 450 GeV lower limit [15] on the t' mass in the semileptonic channel ($pp \to t'\overline{t'} \to [W^+]_{hadronic}\, b\, [W^-]_{leptonic}\, \overline{b} \to \ell \nu b q \overline{q} \overline{b}$) and a 557 GeV lower limit [16] in the dilepton channel, ($pp \to t'\overline{t'} \to [W^+]_{leptonic}\, b\, [W^-]_{leptonic}\, \overline{b} \to \ell^+ \ell^- \nu \overline{\nu} b \overline{b}$). The most recent lower bound on the b' mass are 480 GeV [17] (ATLAS) and 611 GeV [18] (CMS).
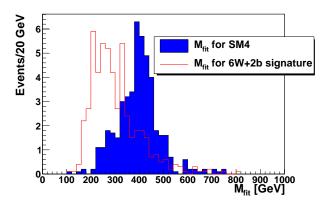

FIG. 18: M_{fit} distribution for the SM4 $2W + 2b \to l\nu b \overline{b} \overline{q} q$ signature (blue) and for the 4G2HDMI $6W + 2b$ signature (red), for a set of 7 TeV LHC events with $\int Ldt = 1\ fb^{-1}$. For both signatures $m_{t'} = 450\ GeV$ is assumed. The peak of the distribution of M_{fit} for the SM4 signature is around $m_{t'}$, while for the new signature the peak is shifted to a significantly lower value coinciding with the peak of the $\overline{t}t$ background. Figure taken from [101].

These searches assumed $Br\,(t' \to bW^+) \sim \mathcal{O}\,(1)$, as expected within the SM4 framework. As was argued above, this is quite unlikely to be the case in models with more that one Higgs doublet, for which new decay patterns can emerge from the interaction of the heavy quarks with the extended Higgs sector, e.g. $t' \to ht$ ($b' \to hb$), $t' \to H^+ b$ ($t' \to H^+ b$). In addition, the SM4 forbidden channels $t' \to b'W$ and $b' \to t'W$, depending on the mass hierarchy in the fourth generation doublet, may no longer be in contradiction with the EWPD if there are more Higgs doublets (see [39] and section III), and may be kinematically open as well. Taking into account such possible new decay modes to the neutral and charged scalars, one can define the generic signature [101]: $t'\overline{t'}/b'\overline{b'} \to n_W W + n_b b$, with n_W and n_b being the number of W and b and $\overline{b}$ jets in the event, respectively.
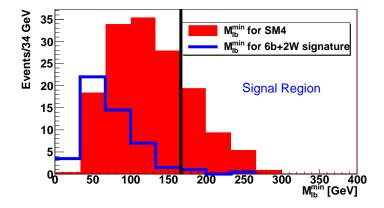

FIG. 19: M_{lb}^{min} for the SM4-like $pp \to t'\overline{t'} \to 2W + 2b$ signature (red) and for the 4G2HDMI $pp \to t'\overline{t'} \to 2W + 6b$ signature (blue) with $m_{t'} = 350\ GeV$ for a set of 7 TeV LHC events with $\int Ldt = 5\ fb^{-1}$ in the dilepton channel. The black line is plotted at the top mass and the region to the right of this line is the "signal region". Figure taken from [101]. .

Focusing on the t' case, [102] have reinterpreted the ATLAS b' search (reported in [17]) to extract limits on t' if it

decays via non-SM4 channels such $t' \to th$ and $t' \to tZ$, whereas [101] have considered, more specifically, the decay channels $t'\bar{t}' \to 6W + 2b$ and $t'\bar{t}' \to 2W + 6b$, as representatives of such new signatures beyond the SM4. As was indeed demonstrated in both [101] and [102], when $t' \to bW$ and $b' \to tW$ are no longer the leading decay channels, the attempts to impose the SM4-motivated dynamics on processes with a completely different topology result in a relaxed limit on the fourth generation quarks with respect to the SM4 case. Specifically, for the t', the CMS analysis in the semileptonic channel was based on the complete reconstruction of each $\ell\nu bq\bar{q}\bar{b}$ event (including the reconstruction of the hadronic W). The total distribution of M_{fit} (the reconstructed mass of the t') and H_T (the scalar sum of all transverse momenta in the event) was used to set a bound on the t' mass. On the other hand, for the new signatures (e.g., $t' \to th$), the number of jets in each event is higher (for example, in the $2W + 6b$ signature, there are 8 jets in the semileptonic channel) and the reconstruction will miss a large part of them, resulting in H_T and M_{fit} being substantially lower - peaking around the main $t\bar{t}$ background. An example of this effect is plotted in Figure 18.
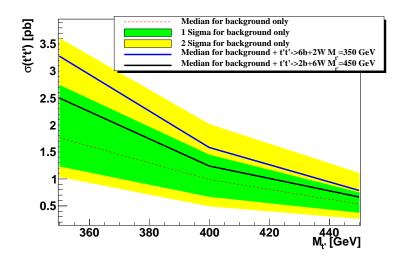

FIG. 20: *The 95% CL exclusion plot distribution on the t' mass assuming the SM4 signature in the semileptonic channel $(1\ell + nj + \not{E}_T)$. For the case of background only, the red doted line is the median and the yellow and green bands are the ± 1 and ± 2 standard deviations accordingly. The black line is the median for background $+ t'\bar{t}' \to 2b + 6W$ with $m_{t'} = 450$ GeV and the blue line is the median for background $+ t'\bar{t}' \to 6b + 2W$ with $m_{t'} = 350$ GeV. The curves for the 4G2HDMI signatures with $m_{t'} = 350 - 450$ GeV lie between these two lines. Figure taken from [101].*

The analysis in the dilepton channel relies on the fact that M_{lb}, which is the invariant mass of a pair of any lepton and a b-jet in the event, is much higher in the underlying $t'\bar{t}'$ signal with respect to the leading $t\bar{t}$ background. In particular, in the case of $t\bar{t}$, M_{lb} has an upper bound that corresponds to the mass of the top quark, and therefore in the region above ~ 170 GeV (the "signal region") M_{lb} is a clean signal of the SM4-like $t'\bar{t}'$ production. However, this dilepton search strategy will fail for signatures with more than 2 leptons or b-jets, as in the case of the 4G2HDMI $2W + 6b$ and $6W + 2b$ signatures, since the combinatorial background will lower M_{lb}, resulting in much less events in the signal region. An example for this effect is plotted in Figure 19.

Assuming now that the physics which underlies the 4th generation dynamics goes beyond the SM4, one can estimate the extent to which the new signatures are already excluded by the current LHC searches [101, 102]. Here we will briefly recapitulate the analysis performed in [101] for both the semileptonic and dilepton channels mentioned above. For the semileptonic channel, [101] demonstrated, using a naive simulation of the new beyond SM4 signals in question, what the exclusion plot would be (using the CMS search strategy which is based on the SM4 $t' \to bW$ decay topology) if the data contains in it the 4G2HDMI signals. This was done by "injecting" $t'\bar{t}' \to 6b + 2W$ events with $m_{t'} = 350$ GeV and $t'\bar{t}' \to 2b + 6W$ events with $m_{t'} = 450$ GeV. The results are shown in Figure 20, which shows that the expected exclusion curves for the background $+ t'\bar{t}' \to 6b + 2W$ and background $+ t'\bar{t}' \to 2b + 6W$ cases are less than 2σ apart from the background only curve. The curves for the 4G2HDMI signatures with $m_{t'} = 350 - 450$ GeV lie between the two signal curves shown in the figure. Thus, using the CMS analysis one would not be able to differentiate between the no-signal and the 4G2HDMI signal scenarios within 2σ, so that we expect the bound on the t' mass within the 4G2HDMI framework to be no larger than about 400 GeV in the semileptonic channel. This result is consistent with the most stringent existing limit, $m_{t'} > 423$ GeV, calculated in [102] by using templates from the b' search at ATLAS [17] and assuming that $\mathrm{BR}(t' \to th) \sim 1$.

For the dilepton channel, the number of events with M_{lb}^{min} in the signal region is negligible for $m_{t'} = 350$ GeV
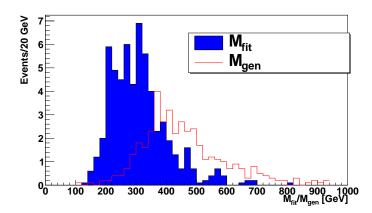
FIG. 21: *Comparison between $M_{fit} = m(l\nu b) = m(q\bar{q}b)$ - the reconstructed t' mass using the CMS method - (in blue) and $M_{gen} = m(Left\ Side) = m(Right\ Side)$ - the reconstructed t' mass using the method suggested in [101] - (in red), for the $pp \to t'\overline{t'} \to 2W + 6b$ signature with $m_{t'} = 450\ GeV$ at the LHC with a c.m. of $7\ Tev$ and $\int Ldt = 1\ fb^{-1}$, in the semileptonic channel $(1\ell + nj + \not{E}_T)$. See also text. Figure taken from [101].*

(the lowest mass considered in the CMS analysis) and even less than that for higher $m_{t'}$ (see Figure 19). One can, therefore, conclude that the CMS dilepton analysis is completely irrelevant for the 4G2HDMI signatures.

As was suggested in [101], an analysis that uses a more general reconstruction method could avoid the kinematic misrepresentation of the beyond SM4 events in both the semileptonic and dilepton channels, and thus yield a higher sensitivity to NP (beyond the SM4) events containing the 4th generation fermions. An example of that is plotted in Figure 21 for the semileptonic channel, which shows how the misconstruction of the t' mass can be surmounted.

VII.   IMPLICATIONS FOR DIRECT SEARCHES OF THE HIGGS

The recently observed new Higgs-like particle with a mass of ~ 125 GeV (at the level of $\sim 5\sigma$, see [20, 21]) is the first potential evidence for a Higgs boson which can be consistent with the SM picture. Furthermore, a study of the combined Tevatron data has revealed a smaller broad excess in the $b\bar{b}W$ channel, which can be related to the production of hW with a Higgs mass between 115 GeV and 135 GeV [22]. These searches further exclude a SM Higgs with masses between $\sim 130 - 600$ GeV.

The quantity that is usually being used for comparison between the LHC and Tevatron results and the expected signals in various models is the ratio:

$$R_{XX}^{Model(Obs)} = \frac{\sigma\left(pp/p\overline{p} \to h \to XX\right)_{Model(Obs)}}{\sigma\left(pp/p\overline{p} \to h \to XX\right)_{SM}}\ , \tag{61}$$

which is the observed ratio of cross-sections, i.e., the signal strengths R_{XX}^{Obs}, and the errors in the different channels are [20–22]:[1]

- $VV \to h \to \gamma\gamma$: 2.2 ± 1.4 (taken from $\gamma\gamma + 2j$)

- $gg \to h \to \gamma\gamma$: 1.68 ± 0.42

- $gg \to h \to WW^*$: 0.78 ± 0.3

- $gg \to h \to ZZ^*$: 0.83 ± 0.3

- $gg \to h \to \tau\tau$: 0.2 ± 0.85

---

[1] We combine the results from the CMS and ATLAS experiments (for $pp/p\overline{p} \to hW \to b\bar{b}W$ we combine the results from CMS and Tevatron), where in cases where the measured value was not explicitly given we estimate it from the published plots.

- $pp/p\overline{p} \to hW \to b\overline{b}W$: 1.8 ± 1.5

One can easily notice that the channels which have the highest sensitivity to the Higgs signals and contributed the most to the recent 125 GeV Higgs discovery are $h \to \gamma\gamma$ and $h \to ZZ^*, WW^*$. In all other channels the results are not conclusive, and at this time, they are consistent with the background only hypothesis at the level of less than 2σ.

As was shown recently in [26], the above reported measurements are not compatible with the SM4 at the level of 5σ. In particular, light Higgs production through gluon fusion is enhanced by a factor of ~ 10 in the SM4 due to the contribution of diagrams with t' and b' in the loops, which in general leads to larger signals (than what was observed at the LHC) in the $h \to ZZ/WW/\tau\tau$ channels. For a light Higgs with a mass $m_h < 150$ GeV and 4th generation masses of $\mathcal{O}(600)$ GeV, $h \to ZZ/WW$ is in fact suppressed by a factor of ~ 0.2 due to NLO corrections [103, 104], and the exclusion is based mainly on the $\tau\tau$ channel. In the $h \to \gamma\gamma$ channel there is also a substantial suppression of $\mathcal{O}(0.1)$ due to (accidental) destructive interference in the loop [55, 105] and another $\mathcal{O}(0.1)$ factor due to NLO corrections [103, 104]. If ν_4 is taken to be light enough, then $Br(h \to \nu_4\nu_4)$ becomes $\mathcal{O}(1)$, suppressing all the other channels and the exclusion gets eased. This, however, further suppresses the $\gamma\gamma$ channel to the level that the observed excess can no longer be accounted for [24]. Therefore, as was also noted in [24, 25, 106], the SM4 is strongly disfavored for any m_{ν_4}, even without considering the $\tau\tau$ channel.
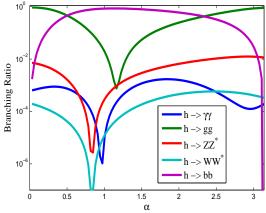

FIG. 22: *The relevant branching ratios of h in the 4G2HDMI, as a function of α, with $m_h = 125$ GeV, $M_{4G} = 400$ GeV, $\epsilon_t = 0.5$ and $\tan\beta = 1$. Figure taken from [109].*

The comparison to any given model can be performed using a χ^2 fit defined as:

$$\chi^2 = \sum_X \frac{\left(R_{XX}^{Model} - R_{XX}^{Obs}\right)^2}{\sigma_{XX}^2} , \tag{62}$$

where σ_{XX} are the errors on the observed cross-sections and R_{XX}^{Model} is calculated using the program Hdecay [108] with recent NLO contributions (which also include the heavy 4th generation fermions for the 4th generation scenarios). One can take advantage of the fact that $\frac{\sigma(YY \to h)_{Model}}{\sigma(YY \to h)_{SM}} = \frac{\Gamma(h \to YY)_{Model}}{\Gamma(h \to YY)_{SM}}$, and calculate R_{XX}^{Model} using

$$R_{XX}^{Model} = \frac{\Gamma(h \to YY)_{Model}}{\Gamma(h \to YY)_{SM}} \cdot \frac{Br(h \to XX)_{Model}}{Br(h \to XX)_{SM}} , \tag{63}$$

where $YY \to h$ is the Higgs production mechanism, i.e., either by gluon fusion $gg \to h$, vector boson fusion $WW/ZZ \to h$ or associated Higgs-W production, $W^* \to hW$ at Tevatron.

In multi-Higgs 4th generation frameworks, the picture becomes more complicated, since there are new scalar states with new Yukawa couplings depending on $\tan\beta$ and α (α is the mixing angle in the neutral Higgs sector), as well as couplings to the W and the Z bosons which are proportional to $\sin(\alpha - \beta)$ and $\cos(\alpha - \beta)$ (with the exception of the pseudoscalar A which does not couple at tree-level to the W and the Z). Furthermore, the specific Yukawa structure can vary depending on the type of the multi-Higgs model, e.g., for the 4G2HDMI case considered below there is an additional parameter, ϵ_t, which parameterizes the $t_R - t'_R$ mixing (see section II and [39]). In Fig. 22 we plot the branching ratios of h as a function of α in the 4G2HDMI, for $m_h = 125$ GeV, $\tan\beta = 1$, $\epsilon_t = 0.5$ and $M_{4G} = m_{t'} = m_{b'} = m_{l_4} = m_{\nu_4} = 400$ GeV.

Let us now examine how well the the 2HDM scenarios with a 4th generation of fermions fit the measured Higgs mediated cross-sections listed above with $m_h = 125$ GeV. The simplest case to study is the "standard" 2HDMII (i.e.,

the 2HDM of type II extended to include a fourth fermion family) with the pseudoscalar A being the lightest scalar, since its couplings do not depend on α [43, 44]. However, as was already noted in [44], for the "standard" 2HDMII the case of a light A decaying to the $\gamma\gamma$ mode is excluded when all 4th generation fermions are heavy. With the new results, in particular, the signals of the 125 GeV Higgs decaying into a pair of vector bosons, the case of the A being the lightest scalar is excluded irrespective of the 4th generation fermion masses.
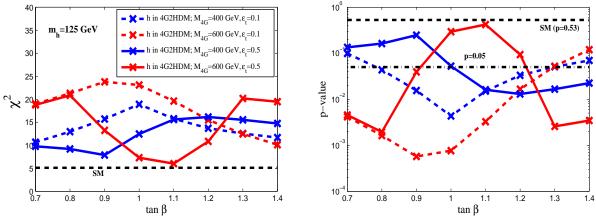

FIG. 23: χ^2 (left plot) and p-values (right plot), as a function of $\tan\beta$, for the lightest 4G2HDMI CP-even scalar h, with $m_h = 125$ GeV, $\epsilon_t = 0.1$ and 0.5 and $M_{4G} \equiv m_{t'} = m_{b'} = m_{l_4} = m_{\nu_4} = 400$ and 600 GeV. The value of the Higgs mixing angle α is the one which minimizes χ^2 for each value of $\tan\beta$. The SM best fit is shown by the horizontal dashed-line and the dash-doted line in the right plot corresponds to $p = 0.05$ and serves as a reference line. Figure taken from [109].
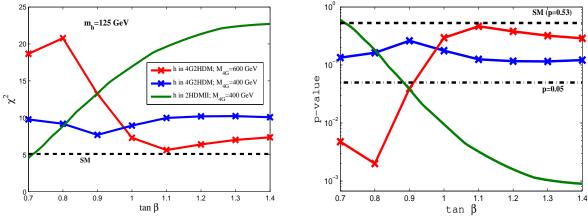

FIG. 24: Same as Figure 23, where here we minimize with respect to both ϵ_t and α for each value of $\tan\beta$. Also shown are the χ^2 and p-values for a 125 GeV Higgs in the SM and in the type II 2HDM with a 4th generation of fermions (denoted by 2HDMII). Figure taken from [109].

Here we wish to extend the previous analysis made for the 2HDMII scenario by calculating the χ^2 for the light Higgs with a mass $m_h = 125$ GeV, both for the 4G2HDMI of [39] and for the 2HDMII with a 4th generation of fermions, and to compare it to the SM. We follow the analysis in [109], which used the latest version of Hdecay [108], where all the relevant couplings for the 4G2HDMI and for the 2HDMII frameworks were inserted. For the treatment of the NLO corrections to $h \to VV$, [109] used the approximation of a degenerate 4th generation spectrum, where two cases were studied: $m_{t'} = m_{b'} = m_{\ell_4} = m_{\nu_4} \equiv M_{4G} = 400$ and 600 GeV (while the first case, i.e., $M_{4G} = 400$, is excluded for the SM4, it is not necessarily excluded for the 2HDM setups, as discussed in the previous section). Note that the 4th generation neutrino is taken to be heavy enough, so that the decays of the light Higgs into a pair of ν' are not considered, thus limiting the discussion to the effects of the altered Higgs couplings in the 2HDM frameworks with respect to the SM4.

Indeed, [109] found that the best fit is obtained for the light CP-even Higgs, h, whereas the other neutral Higgs particles of the 2HDM setups, i.e., H and A, cannot account for the observed data.

The resulting χ^2 and p values in the 4G2HDMI case (combining all the six reported Higgs decay channels above),

with $m_h = 125$ GeV, $M_{4G} = 400$ and 600 GeV, $\epsilon_t = 0.1$ and 0.5 and for $0.7 < \tan\beta < 1.4$ (this range is roughly the EWPD and flavor physics allowed range in these 2HDM setups, see section III) are shown in Fig. 23. The value of the Higgs mixing angle α is the one which minimizes the χ^2 for each value of $\tan\beta$. The SM best fit is also shown in the plot. In Fig. 24 we further show the resulting χ^2 and p-values as a function of $\tan\beta$, this time minimizing for each value of $\tan\beta$ with respect to both α and ϵ_t (in the 4G2HDMI case). For comparison, we also show in Fig. 24 the χ^2 and p-values for a 125 GeV h in the 2HDMII with a 4th generation and in the SM.

Looking at the p-values in Figs. 23 and 24 (which "measure" the extent to which a given model can be successfully used to interpret the Higgs data in all the measured decay channels) we see that, h of the 4G2HDMI with $\tan\beta \sim \mathcal{O}(1)$ and $M_{4G} = 400 - 600$ GeV is a good candidate for the recently observed 125 GeV Higgs, giving a fit comparable to the SM fit. This conclusion is not changed by explicitly adding the EWPD as an additional constraint to the above analysis (i.e., the p-values stay roughly the same, see [109]). The "standard" 2HDMII setup with $M_{4G} = 400$ GeV is also found to be consistent with the Higgs data in a narrower range of $\tan\beta \lesssim 0.9$. Also, the fit favors a large $t - t'$ mixing parameter ϵ_t, implying $\mathrm{BR}(t' \to th) \sim \mathcal{O}(1)$ which completely changes the t' decay pattern [39] and, therefore, significantly relaxing the current bounds on $m_{t'}$ (see previous section).

However, more data is required to effectively distinguish between the 4G2HDMI scalars and the SM Higgs. In particular, in Fig. 25 we show the individual pulls and the signal strengths for the best fitted h signals (i.e., with $m_h = 125$ GeV) in the 4G2HDMI with $M_{4G} = 400$ GeV. We can see that appreciable deviations from the SM are expected in the channels $gg \to h \to \tau\tau$, $VV \to h \to \gamma\gamma$ and $hV \to bbV$. In particular, the most notable effects are about a 1.5σ deviation (from the observed value) in the VBF diphoton channel $VV \to h \to \gamma\gamma$ and a $2 - 2.5\sigma$ deviation in the $gg \to h \to \tau\tau$ channel. The deviations in these channels are in fact a prediction of the 4G2HDMI strictly based on the current Higgs data, which could play a crucial role as data with higher statistics becomes available. They can be understood as follows: the channels that dominate the fit (i.e., having a higher statistical significance due to their smaller errors) are $gg \to h \to \gamma\gamma, ZZ^*, WW^*$. Thus, since the $gg \to h$ production vertex is generically enhanced by the t' and b' loops, the fit then searches for values of the relevant 4G2HDMI parameters which decrease the $h \to \gamma\gamma, ZZ^*, WW^*$ decays in the appropriate amount. This in turn leads to an enhanced $gg \to h \to \tau\tau$ (i.e., due to the enhancement in the $gg \to h$ production vertex) and to a decrease in the $VV \to h \to \gamma\gamma$ and $p\bar{p}/pp \to W \to hW \to bbW$, which are independent of the enhanced ggh vertex but are sensitive to the decreased VVh one. It is important to note that some of the characteristics of these "predictions" can change with more data collected.

Finally, [109] also finds that for the best fitted 4G2HDMI case, the heavier CP-even scalar, H, is excluded by the current data (in particular by the ZZ and WW searches) up to $m_H \sim 500$ GeV, whereas a CP-odd state, A, as light as 130 GeV is allowed by current data (for more details see [109]).
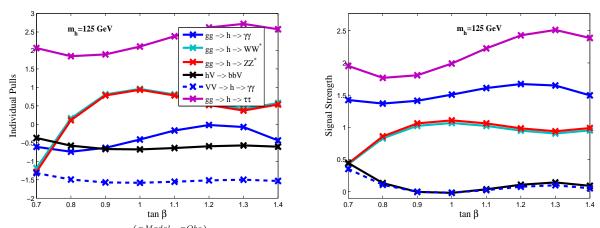

FIG. 25: *The individual pulls $\frac{\left(R_{XX}^{Model} - R_{XX}^{Obs}\right)}{\sigma_{XX}}$ (left plot), and the signal strengths R_{XX}^{Model} (right plot), in the different channels, that correspond to the best fitted 4G2HDMI curve with $m_h = 125$ GeV and $M_{4G} = 400$ GeV, shown in Fig. 24. Figure taken from [109].*

VIII.   SUMMARY

We have addressed several fundamental and challenging questions (that we have outlined in the introduction) regarding the nature and underlying dynamics of the physics and phenomenology of 4th generation fermions, if they exist. We have argued that:

1. The current stringent bounds on the masses of the 4th generation quarks, i.e., $m_{q'} \gtrsim 400$ GeV, are indicative of NP, possibly of a strongly coupled nature, since such new heavy fermionic degrees of freedom naturally lead to a Landau pole at the nearby TeV-scale, which may be viewed as the cutoff of 4th generation low-energy theories.

2. The fact that the 4th generation fermions must be so heavy is, therefore, of no surprise since their large mass stands out as a strong hint for the widely expected new TeV-scale physics, where the new heavy fermionic states may be considered to be the agents of EWSB.

3. If indeed the 4th generation fermions are linked to strong dynamics and/or to compositeness at the nearby TeV-scale, then one is forced to extend the minimally constructed SM4 framework which is not compatible with this viewpoint and neither with current data. In particular, in this case one should expect the sub-TeV particle spectrum to accommodate several new scalar composites of the 4th family fermions. The challenge in this scenario is to construct a viable theory that can adequately parameterize the physics of TeV-scale compositeness and that will guide us to the detection of these new states at the LHC.

We have, thus, suggested and reviewed a class of 2HDM's - extended to include a 4th family of fermions - that can serve as low-energy effective models for the TeV-scale compositeness scenario, and then analyzed/discussed:

- The constraints on these models from EWPD as well as from low-energy flavor physics.

- The expected new phenomenology and the implications for collider searches of the 4th generation heavy fermions as well as of the multi-Higgs states of these models.

We have found that it is indeed possible to construct a natural 2HDM framework with heavy 4th generation fermions with a mass in the range $400 - 600$ GeV, which is consistent with EWPD and which is not excluded by the recent direct measurements at the current high energy colliders.

In particular, we found that, under the 2HDM frameworks for the 4th generation described in this article, one can

- Relax the current mass bounds on the 4th generation quarks.

- Successfully fit the recently measured 125 GeV Higgs signals, to the parameters of the 2HDM with roughly similar quality of fit as the one achieved for the SM with 3 generations. This result is in sharp contrast to the poor fit obtained with the minimal SM4 setup which is, therefore, excluded.

Finally, we have shown that, if such an extended 4th generation 2HDM setup is realized in nature, then one should expect to observe further hints for the underlying TeV-scale dynamics in direct high energy collider signals involving the 4th generation fermions and the associated new scalars as well as in low energy flavor physics.

[1] P.H. Frampton, P.Q. Hung and M. Sher, Phys. Rept. **330**, 263 (2000).

[2] B. Holdom, W.S. Hou, T. Hurth, M.L. Mangano, S. Sultansoy, G. Unel, talk presented at *Beyond the 3rd SM generation at the LHC era workshop*, Geneva, Switzerland, Sep 2008, arXiv:0904.4698 [hep-ph], published in PMC Phys. **A3**, 4 (2009).

[3] For older literature on the SM4, see: Proceedings of the First (February 1987) and the Second (February 1989) International Symposiums on the *fourth family of quarks and leptons*, Santa Monica, CA, published in Annals of the New York Academy of Sciences, 517 (1987) & 578 (1989), edited by D. Cline and A. Soni.

[4] W.A. Bardeen, C.T. Hill and M. Lindner, Phys. Rev. **D41**, 1647 (1990).

[5] B. Holdom, Phys. Rev. Lett. **57**, 2496 (1986), Erratum-ibid. **58**, 177 (1987); S.F. King, Phys. Lett. **B234**, 108 (1990); C. Hill, M. Luty and E.A. Paschos, Phys. Rev. **D43**, 3011 (1991); P.Q. Hung and G. Isidori Phys. Lett. **B402**, 122 (1997).

[6] B. Holdom, JHEP **0608**, 76 (2006).

[7] P.Q. Hung, Chi Xiong, Nucl.Phys. **B848**, 288 (2011).

[8] W.S. Hou, Chin. J. Phys. **47**, 134 (2009), arXiv:0803.1234 [hep-ph]; W.S. Hou, talk given at *34th International Conference on High Energy Physics (ICHEP 2008)*, Philadelphia, Pennsylvania, July 2008, arXiv:0810.3396 [hep-ph]; S.W. Ham, S.K. Oh, D. Son, Phys. Rev. **D71**, 015001 (2005); G. W.S. Hou, Int. J. Mod. Phys. **D20**, 1521 (2011).

[9] S.W. Ham, S.K. Oh, D. Son, Phys. Rev. **D71**, 015001 (2005); R. Fok, G.D. Kribs, Phys. Rev. **D78**, 075023 (2008).

[10] A. Soni, A. K. Alok, A. Giri, R. Mohanta and S. Nandi, Phys. Lett. **B683**, 302 (2010).

[11] A. Soni, A. K. Alok, A. Giri, R. Mohanta and S. Nandi, Phys. Rev. **D82**, 033009 (2010).

[12] A. J. Buras, B. Duling, T. Feldmann, T. Heidsieck, C. Promberger and S. Recksiegel, JHEP **1009**, 106 (2010).

[13] A. J. Buras, B. Duling, T. Feldmann, T. Heidsieck, C. Promberger and S. Recksiegel, JHEP **1007**, 094 (2010).

[14] W.-S. Hou, M. Nagashima, A. Soddu, Phys. Rev. **D76**, 016004 (2007); M. Bobrowski, A. Lenz, J. Riedl and J. Rohrwild, Phys. Rev. D **79**, 113006 (2009); V. Bashiry, N. Shirkhanghah, K. Zeynali, Phys. Rev. **D80**, 015016 (2009); W. S. Hou and C. Y. Ma, Phys. Rev. **D82**, 036002 (2010); O. Eberhardt, A. Lenz and J. Rohrwild, Phys. Rev. D **82**, 095006 (2010); S. Nandi and A. Soni, Phys. Rev. **D83**, 114510 (2011); A.K. Alok, A. Dighe and D. London, Phys. Rev. **D83**, 073008 (2011) 073008; D. Choudhury, D. K. Ghosh, JHEP **1102**, 033 (2011); R. Mohanta, A.K. Giri, Phys. Rev. **D85**, 014008 (2012); A. Ahmed, I. Ahmed, M.J. Aslam, M. Junaid, M.A. Paracha, A. Rehman, Phys. Rev. **D85**, 034018 (2012).

[15] M.M.H. Luk [on behalf of the CMS collaboration], arXiv:1110.3246v2 [hep-ex].

[16] S. Chatrchyan *et al.* [CMS Collaboration], Phys. Lett. **B716**, 103 (2012).

[17] G. Aad *et al.* [ATLAS Collaboration], Phys. Rev. Lett. **109**, 032001 (2012).

[18] S. Chatrchyan *et al.* [CMS Collaboration], JHEP **1205**, 123 (2012).

[19] See e.g., M.S. Chanowitz, M.A. Furman and I. Hinchliffe, Phys. Lett. **B78**, 285 (1978); *ibid.*, Nucl. Phys. **B153**, 402 (1979); W.J. Marciano, G. Valencia and S. Willenbrock, Phys. Rev. **D 40**, 1725 (1989).

[20] S. Chatrchyan *et al.*, [CMS Collaboration], Phys. Lett. **B716**, 30 (2012); See also, J. Incandela, "Observation of a narrow resonance near 125 GeV in CMS", talk given at the ICHEP 2012, July 4-11th, Melbourne, Australia.

[21] G. Aad *et al.*, [ATLAS Collaboration], Phys. Lett. **B716**, 1 (2012); See also, R. Hawkings, "ATLAS Higgs searches and experiment overview", talk given at the ICHEP 2012, July 4-11th, Melbourne, Australia.

[22] [TEVNPH (Tevatron New Phenomena and Higgs Working Group) and CDF and D0 Collaborations], arXiv:1203.3774 [hep-ex].

[23] The ATLAS Collaboration, note: ATLAS Conference note 2011-135, http://atlas.ch/news/2011/Higgs-note.pdf; S. Chatrchyan *et al.* [CMS Collaboration], Phys. Lett. **B710**, 26 (2012).

[24] A. Djouadi and A. Lenz, Phys. Lett. **B715**, 310 (2012).

[25] E. Kuflik, Y. Nir and T. Volanski, arXiv:1204.1975 [hep-ph].

[26] O. Eberhardt *et al.*, arXiv:1209.1101 [hep-ph].

[27] M. Hashimoto, Phys. Rev. **D81**, 075023 (2010).

[28] S. Bar-Shalom, G. Eilam and A. Soni, Phys. Lett. **B688**, 195 (2010).

[29] A. Dighe, D. Ghosh, R. M. Godbole and A. Prasath, Phys. Rev. **D85**, 114035 (2012).

[30] M. Buchkremer, J.-M. Gerard, F. Maltoni, JHEP **1206**, 135 (2012).

[31] M. Baak *et al.* [the Gfitter Group], Eur. Phys. J. **C72**, 2003 (2012).

[32] P.Q. Hung, C. Xiong, Nucl. Phys. **B847**, 160 (2011).

[33] P.Q. Hung, C. Xiong, Phys. Lett. **B694**, 430 (2011).

[34] K. Ishiwata and M.B. Wise, Phys. Rev. **D83**, 074015 (2011).

[35] A.E.C. Hernandez, C.O. Dib, H.N. Neill and A.R. Zerwekh, JHEP **1202**, 132 (2012).

[36] G. Burdman and L. Da Rold, JHEP **0712**, 86 (2007).

[37] G. Burdman, L. Da Rold, O. Eboli and R.D. Matheus, Phys. Rev. **D79**, 075026 (2009); G. Burdman, L. de Lima and R.D. Matheus, Phys. Rev. **D83**, 035012 (2011).

[38] M. Hashimoto and V.A. Miransky, Phys. Rev. **D81**, 055014 (2010).

[39] S. Bar-Shalom, S. Nandi and A. Soni, Phys. Rev. **D84**, 053009 (2011).

[40] M.A. Luty, Phys. Rev. **D41**, 2893 (1990).

[41] E. De Pree, G. Marshall and M. Sher, Phys. Rev. **D80**, 037301 (2009).

[42] M. Sher, Phys. Rev. **D61**, 057303 (2000).

[43] W. Bernreuther, P. Gonzales and M. Wiebusch, Eur. Phys. J. **C69**, 31 (2010).

[44] John F. Gunion, arXiv:1105.3965 [hep-ph].

[45] X.-G. He and G. Valencia, Phys. Lett. **B707**, 381 (2012).

[46] N. Chen and H. He, JHEP **1204**, 062 2012.

[47] H.-S. Lee and A. Soni, arXiv:1206.6110 [hep-ph].

[48] S. Litsey, M. Sher, Phys. Rev. **D80**, 057701 (2009).

[49] S. Dawson, P. Jaiswal, Phys. Rev. **D82**, 073017 (2010).

[50] R.C. Cotta, J.L. Hewett, A. Ismail, M.-P. Le and T.G. Rizzo, Phys. Rev. **D84**, 075019 (2011).

[51] A. Das and C. Kao, Phys. Lett. **B372**, 106 (1996).

[52] The Review of Particle Physics, K. Nakamura *et al.* [Particle Data Group], J. Phys. **G37**, 075021 (2010).

[53] H.-J. He, N. Polonsky and S. Su, Phys. Rev. **D64**, 053004 (2001).

[54] V.A. Novikov, L.B. Okun, A.N. Rozanov and M.I. Vysotsky, Phys. Lett. **B529**, 111 (2002).

[55] G. D. Kribs, T. Plehn, M. Spannowsky and T. M. P. Tait, Phys. Rev. **D76**, 075016 (2007).

[56] J. Erler and P. Langacker, Phys. Rev. Lett. **105**, 031801 (2010).

[57] M.S. Chanowitz, Phys. Rev. **D79**, 113008 (2009).

[58] M.S. Chanowitz, Phys. Rev. **D82**, 035018 (2010).

[59] M.E. Peskin, T. Takeuchi, Phys. Rev. Lett. **65**, 964 (1990); *ibid.*, Phys. Rev. **D46**, 381 (1992).

[60] L. Bellantoni, J. Erler, J. J. Heckman and E. Ramirez-Homs, e-Print: arXiv:1205.5580 [hep-ph].

[61] See e.g., T. Yanir, JHEP **0206**, 044, (2002); J. Alwall *et al.*, Eur. Phys. J. **C49**, 791 (2007).

[62] M. Misiak *et al.*, Phys. Rev. Lett. **98**, 022002 (2007); U. Haisch and A. Weiler, Phys. Rev. D **76**, 034014 (2007); F. Borzumati, C. Greub, T. Hurth and D. Wyler, Phys. Rev. D **62**, 075005 (2000); M. S. Carena, D. Garcia, U. Nierste and C. E. M. Wagner, Phys. Lett. B **499**, 141 (2001); T. Besmer, C. Greub and T. Hurth, Nucl. Phys. B **609**, 359 (2001); M. Ciuchini, E. Franco, A. Masiero and L. Silvestrini, Phys. Rev. D **67**, 075016 (2003); Erratum-ibid. D **68**, 079901 (2003)]; M. Ciuchini, A. Masiero, L. Silvestrini, S. K. Vempati and O. Vives, Phys. Rev. Lett. **92**, 071801 (2004); G. Degrassi, P. Gambino and P. Slavich, Phys. Lett. B **635**, 335 (2006); M. Ciuchini, A. Masiero, P. Paradisi, L. Silvestrini, S. K. Vempati and O. Vives, Nucl. Phys. B **783**, 112 (2007).

[63] F. Borzumati and C. Greub, Phys. Rev. **D58**, 074004 (1998).

[64] M. Ciuchini, G. Degrassi, P. Gambino and G. F. Giudice, Nucl. Phys. **B527**, 21 (1998); *ibid*, Nucl. Phys. **B534**, 3 (1998).

[65] G. Degrassi, P. Gambino and G. F. Giudice, JHEP **0012**, 009 (2000).

[66] A. Ali, E. Lunghi, C. Greub and G. Hiller, Phys. Rev. D **66**, 034002 (2002).

[67] T. Hurth, G. Isidori, J. F. Kamenik and F. Mescia, Nucl. Phys. B **808**, 326 (2009).

[68] C. Greub, T. Hurth and D. Wyler, Phys. Rev. **D54**, 3350 (1996); A.J. Buras, A. Czarnecki, M. Misiak and J. Urban, Nucl. Phys. **B611**, 488 (2001).

[69] K. G. Chetyrkin, M. Misiak and M. Munz, Phys. Lett. **B400**, 206 (1997); [Erratum-ibid. **B425**, 414 (1998)].

[70] A. Ali and C. Greub, Phys. Lett. **B361**, 146 (1995).

[71] N. Pott, Phys. Rev. **D54**, 938 (1996).

[72] M. Misiak and M. Munz, Phys. Lett. **B344**, 308 (1995).

[73] K. Adel and Y. P. Yao, Phys. Rev. **D49**, 4945 (1994); C. Greub and T. Hurth, Phys. Rev. **D56**, 2934 (1997); A.J. Buras, A. Kwiatkowski and N. Pott, Nucl. Phys. **B517**, 353 (1998).

[74] M. Czakon, U. Haisch and M. Misiak, JHEP **0703**, 008 (2007).

[75] C. Bobeth, M. Misiak and J. Urban, Nucl. Phys. **B574**, 291 (2000).

[76] K.G. Chetyrkin, M. Misiak and M. Münz, Phys. Lett. **B400**, 206 (1997), [Erratum-ibid. Phys. Lett. **B425**, 414 (1998)].

[77] M. Misiak, arXiv:0808.3134 [hep-ph].

[78] M. Misiak *et al.*, Phys. Rev. Lett. **98**, 022002 (2007).

[79] D. Asner *et al.*, The Heavy Flavor Averaging Group, arXiv:1010.1589 [hep-ex].

[80] A. Lenz and U. Nierste, arXiv:1102.4274 [hep-ph];

[81] E. Gamiz, C. T. H. Davies, G. P. Lepage, J. Shigemitsu and M. Wingate [HPQCD Collaboration], Phys. Rev. **D80**, 014503 (2009).

[82] E. Gamiz, private communication.

[83] A. J. Buras, M. Jamin and P. H. Weisz, Nucl. Phys. **B347**, 491 (1990).

[84] T. Kinoshita and M. Nio, Phys. Rev. **D70**, 113001 (2004); T. Kinoshita and M. Nio, Phys. Rev. **D73**, 013003 (2006); T. Kinoshita and M. Nio, Phys. Rev. **D73**, 053007 (2006); G. Gabrielse, D. Hanneke, T. Kinoshita, M. Nio and B. C. Odom, Phys. Rev. Lett. **97**, 030802 (2006); T. Aoyama, M. Hayakawa, T. Kinoshita and M. Nio, Phys. Rev. Lett. **99**, 110406 (2007); D. Hanneke, S. Fogwell and G. Gabrielse, Phys. Rev. Lett. **100**, 120801 (2008).

[85] G. Degrassi and G. F. Giudice, Phys. Rev. **D58**, 053007 (1998); A. Czarnecki, W. J. Marciano and A. Vainshtein, Phys. Rev. **D67**, 073006 (2003); S. Heinemeyer, D. Stockinger and G. Weiglein, Nucl. Phys. **B699**, 103-123 (2004); T. Gribouk and A. Czarnecki, Phys. Rev. **D72**, 053016 (2005).

[86] J. Prades, E. de Rafael and A. Vainshtein, arXiv:0901.0306 [hep-ph] (Published in: *Advanced series on directions in high energy physics. 20*); M. Davier *et al.*, Eur. Phys. J. **C66**, 127-136 (2010).

[87] For a recent update, see J. Prades, Acta Phys. Polon. Supp. **3**, 75 (2010), arXiv:0909.2546 [hep-ph].

[88] F. Jegerlehner and A. Nyffeler, Phys. Rept. **477**, 1 (2009); A. Nyffeler, Phys. Rev. D **79**, 073012 (2009).

[89] S. Bar-Shalom, S. Nandi and A. Soni, Phys. Lett. B **709**, 207 (2012).

[90] J. P. Leveille, Nucl. Phys. **B137**, 63 (1978).

[91] J. Adam *et al.* [MEG Collaboration], Phys. Rev. Lett. **107**, 171801 (2011).

[92] A. Dedes, H. K. Dreiner and U. Nierste, Phys. Rev. Lett. **87**, 251804 (2001); C. Bobeth, T. Ewerth, F. Kruger and J. Urban, Phys. Rev. D **66**, 074021 (2002); R. L. Arnowitt, B. Dutta, T. Kamon and M. Tanaka, Phys. Lett. B **538**, 121 (2002).

[93] R. Aaij *et al.* [LHCb Collaboration], Phys. Rev. Lett. **108**, 231801 (2012).

[94] S. Chatrchyan *et al.* [CMS Collaboration], JHEP **1204**, 033 (2012).

[95] A. G. Akeroyd, F. Mahmoudi and D. M. Santos, JHEP **1112**, 088 (2011).

[96] H. E. Logan and U. Nierste, Nucl. Phys. B **586**, 39 (2000).

[97] UTfit collaboartion, see http://www.utfit.org/UTfit/.

[98] M. Antonelli *et al.*, Phys. Rept. **494**, 197 (2010).

[99] K. Kiers and A. Soni, Phys. Rev. D **56**, 5786 (1997).

[100] J.P. Lees *et al.* [BaBar Collaboration], Phys. Rev. Lett. **109**, 101802 (2012); see also G. W.-S. Hou, arXiv:1207.7275 [hep-ph].

[101] M. Geller, S. Bar-Shalom and G. Eilam, Phys. Lett. **B715**, 121 (2012).

[102] K. Rao and D. Whiteson, Phys. Rev. **D86**, 015008 (2012); *ibid*, arXiv:1203.6642 [hep-ex].

[103] G. Passarino, C. Sturm and S. Uccirati, Phys. Lett. **B706** 195-199 (2012).

[104] A. Denner *et. al.*, Eur. Phys. J. **C72**, 1992 (2012).

[105] G. Guo, B. Ren and X.-G. He, arXiv:1112.3188 [hep-ph].

[106] O. Eberhardt *et. al.*, Phys. Rev. **D86**, 013011 (2012).

[107] O. Eberhardt, A. Lenz, A. Menzel, U. Nierste and M. Wiebusch, arXiv:1207.0438 [hep-ph].

[108] A. Djouadi, J. Kalinowski and M. Spira, Comput. Phys. Commun. **108**, 56 (1998), with contributions from arXiv:hep-ph/9704448 [hep-ph].

[109] M. Geller, S. Bar-Shalom, G. Eilam and A. Soni, arXiv:1209.4081 [hep-ph].